Mid-late holocene accretional history of low-lying, coral-reef rim islets, South-Marutea Atoll, Tuamotu, central South Pacific: The key role of marine hazard events

Lucien F Montaggioni, Bernard Salvat, Edwige Pons-Branchu, Arnaud Dapoigny, Bertrand Martin-Garin, Gilbert Poli, Jean-Marc Zanini, Robert Wan

Journal Pre-proof

Mid-late holocene accretional history of low-lying, coral-reef rim islets, South-Marutea Atoll, Tuamotu, central South Pacific: The key role of marine hazard events

Lucien F. Montaggioni, Bernard Salvat, Edwige Pons-Branchu, Arnaud Dapoigny, Bertrand Martin-Garin, Gilbert Poli, Jean-Marc Zanini, Robert Wan

PII: S2666-5921(23)00018-5

DOI: https://doi.org/10.1016/j.nhres.2023.02.004

Reference: NHRES 77

To appear in: *Natural Hazard Research*

Received Date: 31 October 2022

Revised Date: 19 January 2023

Accepted Date: 20 February 2023

Please cite this article as: Montaggioni, L.F., Salvat, B., Pons-Branchu, E., Dapoigny, A., Martin-Garin, B., Poli, G., Zanini, J.-M., Wan, R., Mid-late holocene accretional history of low-lying, coral-reef rim islets, South-Marutea Atoll, Tuamotu, central South Pacific: The key role of marine hazard events, *Natural Hazard Research* (2023), doi: https://doi.org/10.1016/j.nhres.2023.02.004.

Mid-Late Holocene accretional history of low-lying, coral-reef rim islets, South-Marutea Atoll, Tuamotu, central South Pacific: the key role of marine hazard events

Lucien F. Montaggioni [a]*, Bernard Salvat [b], Edwige Pons-Branchu [c], Arnaud Dapoigny [c], Bertrand Martin-Garin [a], Gilbert Poli [d], Jean-Marc Zanini [e], Robert Wan [f].

[a] Aix Marseille Univ, CNRS, IRD, INRAE, CEREGE, 13331 Marseille, France

[b] PSL-École pratique des hautes études, UAR 3278, EPHE, CNRS, UPVD, Labex Corail,

[c] LSCE/IPSL, CEA–CNRS–UVSQ, Université Paris-Saclay, 91198 Gif-sur-Yvette, France

[d] Environmental Consultant 75016 Paris, France

[e] Environmental Consultant 75014 Paris, France

[f] Tahiti Perles, Papeete, BP 850, French Polynesia

Corresponding author, Email address: montaggioni@cerege.fr

Abstract

South-Marutea Atoll is located at the south-eastern end of the Tuamotu Archipelago, French Polynesia, central South Pacific. Understanding the modalities of islet building from low-lying atolls over the mid to late Holocene, in relation to sea-level changes and cycles of marine hazard events, is a prerequisite for better anticipate future geomorphic changes to which the islets will likely be faced in the next decades under global climate warming. Herein is presented the depositional history of two selected atoll islets, based on chronostratigraphic analysis of sedimentary, coral-dominated sequences from six excavations. Identified as Motu Aramu and Motu Vainono, these islets are located respectively in north-north-east and due south of the atoll rim. Additional surficial sampling was conducted on modern ocean-facing

shingle ridges, respectively on north-north-west (Motu Oire), west (Motu Aranui) and east (Motu Tekava) rim areas, in order to date the latest ridge-emplacement stages. Oire and Aranui sites, located along the leeward atoll sites, are protected from trade winds, Aramu, Vainono and Tekava are located on the windward sides, directly exposed to northeasterly and southeasterly storm swells respectively. A total of 88 coral clasts were collected to be U/Th dated. The excavated sequences range between 2.50 m and 0.90 m in thickness, from the outer islet sides lagoonwards. Five lithofacies, including two subfacies, were recognized based on texture and biological composition: a coral boulder-cobble-dominated, a coral pebble-dominated – pebble-supported and sand-supported subfacies – and a foraminifera-rich, sand-dominated and an organic-rich, pebble to sand facies. These facies tend to be distributed from ocean sides landwards according to a decreasing grain-size gradient. A model of atoll-island accretion emerges in relation with changes in frequency and intensity of marine hazard events. The islet foundations consist of conglomerate platforms, locally up to 1.0 m thick, deposited from about 5,000 to 1,000 yr BP. Islets began to accrete from 5,000 yr BP. While at Motu Vainono, islet building occurred continuously over the last 5,000 years, at Motu Aramu, there is an apparent non-depositional episode, from 4,000 to 2,000 yr BP, interpreted as caused by a marked decreased in ENSO-related cyclone activity. The outer shingle ridges in all studied sites were regularly reshaped during the last millennium. During the last 5,000 years, the major accretion-islet episodes occurred irrespective of the course of sea level, indicating that sea-level change was not a driver of islet accretion. Periodical, marine high-energy events clearly appear to be the key controls of islet shaping. Shifts of cyclone source areas further south and increasing cyclone intensity, but lower frequency, due to enhanced ENSO variability throughout the 21st century, is postulated to expose the Gambier island Group to stronger, but fewer disturbance events when compared to the last millennia.

Keywords:

Atoll
Islet accretion
Storminess
Tuamotu
Central south Pacific
Holocene

1. Introduction

According to the lastest IPCC Report (Pörtner et al., 2022), sedimentary coastal systems will be subjected to drastic topographic readjustments prior to the end of the current century in response to ongoing global climate warming. In the Pacific Ocean, low-lying coastal systems are mainly represented by atolls, i.e. shallow-water, annular to elongate, coral-reef rimmed islands, usually overtopped discontinuously by islets, composed of coral-derived rubble and/or skeletal sands (Woodroffe and Biribo, 2011). These islets are known as *motu* by Polynesian natives. Culminating at elevations rarely exceeding +5 m above present mean sea level (pmsl), these have been interpreted as storm-generated, depositional landforms built up during the last millennia in relation with relative changes in sea level (Pirazzoli and Montaggioni, 1986; Dickinson, 2009; Woodroffe et al., 1999; Kench et al., 2005; Barry et al., 2007; Kench et al., 2014a, 2014b).

Over an about twenty-year period, in the Indo-Pacific, a great deal of research was dedicated to understanding the morphological evolution of low-lying atoll islets during the last few decades in response to the rise in sea level (Roy and Connell, 1991; Woodroffe, 2008; Dickinson 2009; Webb and Kench, 2010; Rankey, 2011; Ford, 2012; Yates et al., 2013; Ford and Kench, 2015; Storlazzi et al., 2015; Purkis et al., 2016; Duvat, 2019; Duvat et al., 2017a; Shope and Storlazzi, 2019) and to the intensification of storminess (Kench and Brander, 2006; Hoecke et al., 2013; Canavesio, 2014; Smithers and Hoecke, 2014; Costa et al., 2017; Duvat et al., 2020). The relevant findings were used to attempt predicting the morphodynamic behavior of these islets in the face of global warming in the next future decades. By contrast,

a limited number of investigations were carried out in order to reconstruct the morphological reconstruction of atoll islets during the last millennia (Kench et al., 2014a, b; Montaggioni et al., 2018, 2019).

Atoll islets are usually regarded as potentially vulnerable, liable to experience submersion and/or erosion (Yamano et al., 2007; Woodroffe, 2008; Dickinson, 2009; Ford and Kench, 2014; Canavesio, 2014, 2019; Storlazzi et al., 2015; Shope et al., 2016, 2017; Duvat et al., 2017b; Montaggioni et al., 2021; Amores et al., 2022). As a result, the fate of islets together with the related human settlements, remain uncertain (Shope and Storlazzi, 2019; Magnan et al., 2018, 2022) and therefore is still actively debated. Among scientists, there are those who believe that islets could be submerged (Yamano et al., 2007; Dickinson, 2009; Connell, 2013; Hubbard et al., 2014; Woodruff et al., 2013; Storlazzi et al., 2015), and others who thought that they will persist, migrating laterally across atoll-rim surfaces (Webb and Kench, 2010; Rankey, 2011; Biribo and Woodroffe, 2013; Ford, 2012, 2013; Le Cozannet et al., 2014; Pala, 2014; Ford and Kench, 2015; McLean and Kench, 2015; Duvat and Pillet, 2017; Duvat et al., 2017b). In any case, active cyclogenesis are known to promote both islet accretion and erosion, generally at different sites of a same atoll (Stoddart, 1971; Stoddart and Steers, 1977; Scoffin 1993; Canavesio, 2014; Montaggioni et al., 2018, 2019, 2021).

In French Polynesia, studies were conducted on the dynamics of atoll-islet shorelines in response to change in sea level over the last few decades (Duvat, 2019; Duvat and Pillet, 2017; Duvat et al., 2017a, b). Correlatively, Canavesio (2014, 2019) explored the influence of extreme marine hazards on the short-term evolution of motu morphology. In both cases, the investigations focused on a few atoll sites and atolls only. Furthermore, as claimed by Shope and Storlazzi (2019), such works only based on a few decades of observations may not accurately predicate how atoll islets will react in the future when sea level will reach

98 elevations as high as or higher than those reached during the mid-late Holocene islet accretion
99 phases and, in addition, when storminess will become stronger.

100 Estimating the degree of vulnerability of atoll islets to ongoing climate change requires as a
101 prerequisite detailed reconstructions of the mode and timing of atoll islet formation over
102 millennial timescales. Islet sedimentary beds are known to preserve evidence of the passage
103 of intense storms. In French Polynesia, studies devoted to reconstructing the internal
104 architecture of low-lying islets are still limited to Takapoto (Montaggioni et al., 2018, 2019)
105 and Rangiroa (Montaggioni et al., 2022) Atolls. The findings revealed that, at Takapoto, on
106 both leeward and windward sides, motu have formed over the last 2,500 years, as sea level
107 was falling, from depocentres initially located in the middle parts of the atoll rims, then
108 accreting centrifugally seawards and lagoonwards. By contrast, in northern Rangiroa, islet
109 development appears to have started about 6,000 years ago at the time sea level was moving
110 up to its present position, indicating that the main accretionary phase of the motu has occurred
111 during the rising sea-level episode, approximately from 6,000 to 3,000 years BP. As their
112 islets were demonstrated to have formed at different stages of the sea-level course over the
113 last 6,000 years, the question is to what extent the models from Takapoto and Rangiroa, both
114 located in the northern Tuamotu, are representative at the whole archipelago scale.

115 The present study aims to reconstruct the timing and mode of formation of two rim islets from
116 South-Marutea Atoll (Fig. 1), situated at the south-eastern end of the Tuamotu Archipelago, at
117 a distance of 1500 km and 1300 km from Takapoto and Rangiroa Islands. The selected motu
118 are located in the north and south areas of the atoll respectively. The main objectives are to
119 elucidate if there are potentially time offset in islet initiation and differences in accretional
120 processes between atolls situated at the opposite ends of a same reef province, and suspected
121 to be subjected to differential environmental conditions and storm regimes. Assuming that the

mid to late Holocene sea-level pattern defined from the north-western Tuamotu (Pirazzoli and Montaggioni, 1988a; Hallmann et al., 2020) is of regional value, also applicable to the south-eastern parts of the archipelago (Pirazzoli and Montaggioni, 1987) may lead to isolate the respective roles of sea-level change and marine natural hazard events in South-Marutea atoll-islet formation.

2. Regional setting

2.1. Site location and atoll morphology.

Composed of 77 atolls, the Tuamotu Archipelago is located in the central South Pacific, extending along a west-north-west to east-south-east axis, about 1700 km long. Located at 1470 km from Tahiti, South-Marutea Atoll, also known as Quiros, Lord Hood, Marutea-I-Runga or Nuku-Nui, lies in the far south-eastern part of the archipelago, between 21°28’27.74’’–21°34’25.12’’ latitude south and 135°38’42.57’’–135°27’12.46’’ longitude west (Fig. 1a). This atoll has to be differentiated from North-Marutea, located at about 650 km east of Tahiti. South-Marutea is resting on a 37.3–30.4 million years old, oceanic crust (Müller et al., 1997). Geodynamically speaking, it belongs to the Tuamotu trail chain, presumably generated from the Easter hotspot (Ito et al., 1995), to be distinguished from the nearby Moruroa-Gambier-Pitcairn island chain generated by the Pitcairn hotspot (Dupuy et al., 1993). The South-Marutea volcano, about 2700 m high, is likely to have started erupting by the lower Miocene. Geographically and administratively speaking, rising at a distance of less than 200 km north of Mangareva Island, South-Marutea is part of the Gambier Island Group.

First described by Seurat (1904), South-Marutea is of closed type (totally devoid of passes), broadly trapezoid in shape, 20 km long and 8 km wide, with a circumference of 55 km (Fig. 1b). Its main axis, oriented west-north-west to east-south-east, is consistent with that of the Tuamotu

island chains. The atoll reef rim ranges between about 350 and 1100 m in width, covering about 15 km^2. The lagoon is 112 km^2 in area, –40 m in maximum depth and exhibits a blue hole, –72 m deep, close to its eastern border. A 10 km-long, almost continuous motu occupies the north-eastern rim part while the other rim areas have small islets usually separated by *hoa*, i.e. shallow channels allowing water exchanges between the open sea and the lagoon at high tide. The islets are elongated or crescent-shaped.

The atoll rim is fringed oceanwards by a coral-reef flat zone, 150 to 230 m wide, less than 1 m deep, overlined by an about 0.50 m-high algal crest, at its outermost borders. The living coral cover rate does not exceed 5 % of the total reef-flat surface. The upper forereef zone consists of a gently-dipping spur-and-groove system, followed outwards by a sub-horizontal, about 50 m-wide terrace, usually ending into a drop-off at depths of 10–15 m. The spur-and-groove system and the terrace are colonized by coral communities dominated by pocilloporids and acroporids. Observations from the north-north-west rim tip (Motu Oire), at base of the spurs, living coral coverage averaged 45 % over the past few years (Chancerelle, Y., CRIOBE, pers. com.)

2.2. Climate

In French Polynesia, the climate system is driven by the trade winds and by the El Niño-Southern Oscillation () which regulates both tropical cyclones and extra-tropical storms (Andréfoüet et al., 2012; Lecacheux et al., 2013). In the Gambier Islands, the climate is typically maritime, tropical, humid, but relatively cooler than that from the north-western Tuamotu region. Rainfall remains relatively stable throughout the year, averaging 140 mm in July and 210 mm in November, thus resulting in an average annual rate of 2,000 mm. As in the whole tropical Pacific, the wind regime at South-Marutea, is dominated by trade-winds,

blowing mainly from the north to south-east sectors (Fig. 2). During the winter season, the trade winds generate strong, about 2–2.50 m-high wave surges. During the summer season, the trade winds are significantly less active and generate moderate swells, occasionally disturbed by distant-source storms originating from the southern latitudes (Canavesio, 2019) and cyclones. Tides are semi-diurnal and microtidal, averaging 0.70–0.80 m in amplitude at spring tide.

French Polynesia has clearly fewer cyclones than the rest of the central South Pacific. The cyclone season occurs generally during the austral summer. The eastward shift of warmer waters during El Niño events triggers the motion of tropical storms further east to the Tuamotu. Most cyclones come from the west through the Cook Islands, usually passing south of the Society Islands, but more regularly passing over the Austral Islands (Larrue and Chiron, 2010). Some cyclones generate from within the Marquesas. Increase in ENSO variability is driven by a change in the magnitude and frequency of extreme El Niño events (Bjerknes, 1969; Kao and Yu, 2009). During active, El Niño phases, intense cyclonic hazards mainly affect the region bounded by the Tuamotu and Austral Islands, while, during la Niña phases, decreasing cyclonic activity seem to operate between the Gambier and the southern Austral areas (Laurent and Varney, 2014). As a response to global warming, there was a significant enhancement of ENSO variability by about 25 % over the last five decades, compared to the preindustrial times (Grothe et al., 2019). The province is also affected by tropical lows that form over oceanic areas with surface temperature of about 26 °C, just poleward of the Inter-Tropical Convergence Zone (ITCZ) where the trade winds of northern and southern hemispheres are converging. These can generate strong winds and swells across the Tuamotu province.

In French Polynesia, the history of extreme marine hazard events is poorly documented (Laurent and Varney, 2014; Dupon, 1987). Between 1822 to 2014, about 24 extreme wave events, most interpreted as related to tropical cyclones, would have passed across the region. The last ones were interpreted as triggered by 'Super-ENSO' events (Hameed et al., 2018), presumably in relation to global climate warming. These last events were anomalous since, over periods of several centuries, the number of strong storms and cyclones in the province was expected to probably range between 2–3 per century (Canavesio, pers.comm.) to a maximum of 4–10 (Dupon, 1987). Cyclone events typified by a 50-year return interval would generate wave exceeding 12 m high (Canavesio, 2014).

Storm wave surges hitting South-Marutea are generated by tropical cyclones, depressions, and southern, distant-source wave surges. For the 1831 to 1968 period, there were three recorded passages of destructing cyclones in the Gambier region. Initiated close to the Marquesas Archipelago, all these cyclones were described as having followed similarly close trajectories as tracked south-east along the west Mangareva coasts at distances of less than 10 km (Laurent and Varney, 2014). During the 1969–2010 interval, South-Marutea is known to have been impacted by eight cyclones and depressions (Laurent and Varney, 2014) (Fig. 3). In the vicinity of the Gambier Islands, most cyclones tend to become less powerful, grading into tropical depressions, hence unable to displace the largest coral debris. The most recent damaging effects have resulted from the passage of cyclones Nano and William. Nano passed over South-Marutea by 27th January 1983. All atolls located along its trajectory were impacted, especially their north- and east-facing rim sides which were totally submerged. Descriptions from neighbouring atolls of Hao and Tureia reveal that about 15 to 18 m-high waves have flooded over the reef rims, locally resulting in removing portions of islets over lengths of 60 m and widths of 20 m, together with transport of coral-built mega-blocks from the adjacent forereef slopes onto the motu (Laurent and Varney, 2014). The eye of Cyclone

William has passed close to the north of South-Marutea by 20th April 1983. At Turea, waves of about 8 to 9 m high were observed. It is noteworthy that, at South-Marutea, while there are several metre-thick, outer shingle ridges, mostly composed of coral boulders and cobbles, deposited along the reef-rim, there is no mega-boulder. Large mega-casts are also missing (B. Salvat, pers. observ.).These are striking features because numerous mega-clasts, a few to tens of cubic metres in volume, are frequently present on reef flats in the majority of atolls in the Tuamotu, locally in the north and central part of the archipelago, usually deposited along the northern and southern faces (Bourrouilh and Talandier, 1985; Etienne et al., 2011; Terry and Etienne, 2011; Lau et al., 2016). This strongly suggests that the studied atoll and most of nearby islands have escaped catastrophic impacts generated by the close passage of cyclones, in contrast to what is seen at Hao and Tureia. South-Marutea, located further south, close to the end of the cyclonic tracks in the south Pacific (Larrue and Chiron, 2010; Laurent and Varney, 2014), is likely to have been hit by cyclones with loss of strength. However, mean tide levels during a cyclonic event can be strongly impacted by both wave setup, i.e. increase of mean water level due to waves breaking on the reef front, and by runup, i.e. maximum elevation reached by waves on the atoll land. For cyclonic wave heigths of 8 to 12 m, runup effects could increase the reference ocean water level by more than 4.5–5.0 m along coastlines (Pedreros et al., 2010). It is noteworthy that elevation reached by sea level is sensitive mainly to wave direction. The effects of changing incident waves that deflect into a direction different from the perpendicular to the reef front line could cause increasing risk and disturbances in some areas, especially near passes or hoa. Similarly, atoll-islet inundation can occur from waves surges directly generated from lagoonal waters (Damlamian et al., 2013).

Distant-source swells originate from high-latitude storms, especially in the south (austral) hemisphere. There is little information about the real influence of distant-source storms in atoll shaping in the Tuamotu, although their return frequency is approximatively annual,

241 probably because these have usually limited effect on human activities. However, these are
242 known to have triggered a rise of up to 2.50 m in atoll lagoon level above low spring tide,
243 resulting in islet submergence and damage (Canavesio, 2019). Lagoon water infilling seems
244 to depend not only upon the magnitude of the storm wave event, but also upon the duration of
245 the event.

246 In addition, little is known about the frequency and effects of tsunamis in French Polynesia
247 and, especially, in the south-eastern Tuamotu end (Sladen et al., 2007). Around fifteen
248 tsunamis were estimated to have hit French Polynesia and the Tuamotu since the fifteenth
249 century (Lau et al., 2016). Earthquake-generated tsunamis from the eastern Pacific subduction
250 zones seem to be potentially not able to impact the Gambier areas (Heinrich et al., 1996;
251 Reymond et al., 2013). According to Sladen et al., (2007), the Tuamotu have been
252 significantly less affected by tsunamis than high volcanic islands in other French Polynesian
253 archipelagoes, although some atoll-rim deposits may be interpreted as resulting from
254 devastating tsunami impacts (Montaggioni et al., 2022). Since the 16th century, less than ten
255 tsunamis were expected to have struck the Tuamotu islands and generated less than 2 m-high
256 waves (Lau et al., 2016).

257 Moreover, as emphasized by Duvat et al. (2020), climate events regarded as moderate
258 compared to tropical cyclones can significantly contribute to atoll-islet shaping. Usually
259 overlooked as sediment providers, low-to medium water energy hazards, with return periods
260 of 2–3 years, compared to those of cyclone (several decades), regularly supply motu with
261 material derived from upper forereef and reef-flat zones and contiguous conglomerate
262 platforms.

Rapid, high amplitude mean global sea-level rise is expected for the next centuries (Horton et al., 2020). Highest sea-level positions should be close to those estimated for the last interglacial MIS 5e stage (Rohling et al., 2007; Kopp et al., 2009)..

3. Material and methods

3.1. Field surveys

The studied motu sites are the following: north-east (Aramu) (Fig. 1c), due south (Vainono) (Fig. 1d), west (Aranui) (Fig. 1e), north-north-west (Oire) (Fig. 1f) and due east (Tekava) (Fig. 1g).

First, detailed levelling along longitudinal profiles across the atoll-reef rim was conducted using a conventional automatic level. Each reference point along the profiles was positioned using DGPS coordinates. Elevations were measured by reference to present-day mean sea level (pmsl), assuming a conservative error of ±0.10 m. The profiles across the motu reveal similar protruding relief seawards. These relate to shingle ridges bordering the ocean-facing sides of the atoll-reef rim, as observed at Motu Vainono, across its highest tip (Figs. 1d, 4a) and at Motu Oire (Figs. 1f, 4b). The islets rest usually on conglomerate platforms, i.e. lithified, heterometric skeletal sheets, regarded as cemented within vadose and phreatic marine zones during the sea-level lowering over the last 4,000 years (Montaggioni et al., 2021). Conglomerates are less than 1.00 m in apparent thickness, but are thicker locally, particularly in the south-south-west (Motu Aranui) and the west (Motu Oire) areas of the atoll reef-rim (Fig.5a, b, c). Coral pebbles were collected superficially along the shingle-ridge profiles for radiometric dating submission. Similarly, for comparison, samples were also taken along the ocean-facing shingle ridges on Motu Aranui (Fig. 1e), on the south-south-

285 west coast (21°31’38.6”S, 135°37’48.9”W) and Motu Tekava (Fig. 1g), on the south-south-
286 east atoll-rim end (21°31’51.31’’S, 135°27’23.70’’W).

287 Additional topographic surveys were conducted in relation to excavated cross-sections
288 through two selected islets, respectively Motu Aramu, exposed to the north-north-east trade
289 winds (21°29’00.2’’S, 135°30’48’’W) and Motu Vainono, exposed to the south-east
290 (21°34’05.3’’S, 135°33’05.9’’W). Aramu is 230 m long, while Vainono extends over 720 m.
291 Islet topography are very similar at both studied sites. Along the ocean side, the transition
292 zone between the inner reef-flat zone and the land is occupied by steeply-dipping (up to 20°)
293 sandy, skeletal beaches (Fig. 6). Inland, there are unconsolidated rubble ridges, mainly
294 composed of block-sized (0.30 m on average), individual coral colonies, dominated by
295 pocilloporids and acroporids (Fig. 7). The ocean-facing ridge slopes are steep (up to 30°)
296 while the inner faces are gently-dipping (less than 15°). Ridge heights at the transect sites are
297 2.30 m at Motu Aramu (Fig. 8) and 5.10 m at Motu Vainono (Fig. 9). Behind the ridges, there
298 are gently-dipping (less than 10–15°) to flat-topped benches culminating at elevations of
299 1.60 m to 2.60 m respectively. The benches end into 10° sloping beaches, about 20 to 80 m in
300 width. The inner sides of shingle ridges at Motu Vainono are covered by low-growing plants
301 (*Scaevola taccada*). Conglomerate platforms and beaches from the ocean-facing Aramu areas
302 are colonized by spaced *Pemphis acidula* tufts – *miki-miki* in Polynesian language. The inner,
303 flat-topped surfaces of both islets are occupied by both low-growing plants (*Scaevola*
304 *taccada*, *Microsorum grossum*), shrubs (*Pandanus tectorius)* and trees *(Guettarda speciosa,*
305 *Cocos nucifera).*

306 Second, vertical excavations using backhoe were dug through Motu Aramu (Fig. 8) and Motu
307 Vainono (Fig. 9) from top surface to underlying conglomerate surfaces in order to determine
308 islet subsurface stratigraphy. On both motu, the excavations were dug at three specific

309 locations: just behind the shingle ridge, in the middle part of the motu and on the lagoon-
310 facing margin. From the ocean side inwards, these holes are successively labelled A
311 (21°28'57.1"S, 135°30'45.6"W), B (21°29'00.2"S, 135°30'48.1"W) and C (21°29'02.7"S,
312 135°30'50.3"W) on Motu Aramu, and D (21°34'09.0"S, 135°33'04.2"W), E (21°34'05.3"S,
313 135°33'05.9"W), and F (21°33'57.54"S, 135°33'07.86"W) on Motu Vainono. Field grain-
314 size analysis of coarser detrital material was performed using the Udden-Wentworth
315 classification (Terry and Goff, 2014) as measured along the longest axis from photographed
316 square-metre quadrats. Coral pebbles and gravels were collected for radiometric dating at all
317 excavated sites. Taxonomic identification of dated coral specimens was made at the generic
318 level.

319 *3.2. Uranium–thorium dating procedures*

320 The reconstruction of atoll islet chronostratigraphy and building history is based on uranium-
321 series dating of the 88 coral gravels to pebbles, labelled M, collected on South-Marutea Atoll,
322 both at the surface of islets and, within excavations, along the walls and at the bottom.

323 Prior to radiometric analysis, millimetric pieces of the coral clasts were cut using a micro saw
324 in order to select the most clean and pristine parts. These pieces were rinsed with mQ water
325 and ultra-sonicated several times. After adding a triple ^{229}Th ^{233}Ue ^{236}U spike in a Teflon
326 beaker, samples (from 150 to 350 mg) were dissolved with diluted HCl. The U–Th separation
327 and purification were performed after coprecipitation with $Fe(OH)_3$, on 0.6 ml columns filled
328 with U-TEVA and prefilter resins, in nitric media – see Pons-Branchu et al. (2014) for details.
329 The U and Th isotopic compositions were analyzed at the *Laboratoire des sciences du climat*
330 *et de l'environnement* (LSCE, France), on a Multi-Collector inductively coupled plasma source
331 mass spectrometer (MCeICPMS) Thermo Scientific™ Neptune^{plus} fitted with a desolvating
332 introduction system (aridus II), and a jet interface. For mass fractionation correction, we used

an exponential mass fractionation law – normalized to natural $^{238}U/^{235}U$ isotopic ratio – and standard – sample bracketing. More details on the analytical procedure – chemistry and MC-ICPMS analysis – can be found in Pons- Branchu et al. (2014). After corrections for peak tailing, hydrate interference and chemical blanks, $^{230}Th/^{234}U$ ages were calculated (Table 1) from measured atomic ratios through iterative age estimation using the ^{230}Th, ^{234}U, and ^{238}U decay constants of Cheng et al. (2013) and Jaffey et al. (1971). Ages are expressed in calendar years (cal.yr), by reference to 2022, i.e. the year of sample analysis. In order to make age results more easily comparable to previous research, particularly that based on radiocarbon measurements, ages are also given in conventional years BP by reference to 1950 (see Table 1, Supplementary Material).

3.3. Significance of coral-clast ages

Radiometric dating of displaced skeletal material (corals, molluscs, foraminifera) for reconstructing depositional histories of atoll islets were discussed by Woodroffe et al. (1999, 2007), Kench et al. (2014) and Montaggioni et al. (2018, 2019, 2021, 2022). As an unknown time interval (tens to hundreds of years) is expected to separate the time of death of a given organism from the time of final deposition and stabilisation of its skeletal fragments, islet chronologies have therefore to be interpreted as relative, not absolute. Coral clasts may have experienced successive cycles of displacement, reworking and resedimentation. This is clearly evidenced by a number of age inversions in the stratigraphic sections (Figs. 8, 9). However, islet chronologies is assumed to be consistent, since most of the dated samples occupy a stratigraphic position within the excavations, particularly, within those close to the outer ridges and from the middle parts of both islets, which is in accordance with their age. Samples tend to be younger closer to the surface and older closer to the bottom. In these sites, the youngest ages obtained are regarded to be closer to the time of definitive stabilization of the

relevant islet section. Clast stabilization is believed to have taken place within 200–1,000 yr-long intervals, according to clast ages recorded at base of the excavations.

4. Results

4.1. Expected age of deposition of conglomerate platforms

Ages of coral clasts incorporated into islet-supporting conglomerates, collected from both outcrop surfaces or at the bottom of the excavations vary widely from site to site (Fig. 10). At Motu Aramu, ages range from 3,585 ± 10 cal.yr (M1), 3,593 ± 20 cal.yr (M4), and 4,108 ± 10 cal.yr (M43) to 4,181 ± 8 cal.yr (M52). At Motu Vainono, conglomerate clasts yielded ages of 1,109 ± 4 cal.yr (M16), 1,204 ± 8 cal.yr, (M25), 3,218 ± 7 cal.yr (M118), and 3,986 ± 10 cal.yr (M88). At Motu Aranui, conglomerate ages are among the oldest recorded: 3,665 ± 16 cal.yr (M148) and 4,829 ± 24 cal.yr (M149). By contrast, at Tekava, conglomerate deposits are among the youngest ones: 1,011 ± 32 cal.yr (M103), 1,339 ± 6 cal.yr (M102), and 1,743 ± 7 cal.yr (M101).

4.2. Expected age of deposition of ocean-facing shingle ridges and inner sheet surfaces

U/Th dating of coral clasts collected from the shingle-ridge and inner islet surfaces at the different islet settings suggests that the ridges have been supplied in coral detritus between the last few decades to the last millennia (Fig. 10). Clast deposition has taken place decades to century apart depending on exposure to wave surges and local forereef slope physiography of each considered atoll site. The youngest ages are mostly obtained from the outermost, ocean-facing ridge surfaces or tips: Aranui (47 ± 4 cal.yr, M138), Aramu (51 ± 2 cal.yr, M53), Vainono (79 ± 2 cal.yr, M19; 185 ± 3 cal.yr, M18), Oire (304 ± 3 cal.yr, M162; 308 ± 5 cal.yr, M164), Tekava (343 ± 4 cal.yr, M107). By contrast, samples from the inner talus, just behind the ridge tips, provide ages significantly older: Tekava (862 ± 5 cal.yr,

M100), Oire (1,255 ± 11 cal.yr, M166; 3,565 ± 13 cal.yr, M167), Vainono (2,314 ± 150 cal.yr, M21; 2,678 ± 9 cal.yr, M24; 2,695 ± 8 cal.yr, M22).

Ages of samples from the inner sheet surfaces range are the following (Fig. 10): 108 ± 3 cal.yr, (M44) and 1,786 ± 12 cal.yr (M26) at Aramu, 2,480 ± 10 cal.yr (M132), 42 ± 2 cal.yr (M65) and 2,885 ± 8 cal.yr (M85) at Vainono, 3,846 ± 15 cal.yr (M109) at Tekava.

4.3. Internal islet structure and lithostratigraphy

Examination of the excavations dug through both Motu Aramu and Motu Vainono revealed that the relevant unconsolidated deposits are resting on firmly indurated, conglomerate pavements. The conglomerate top surfaces range from 0.40 to 0.70 m (0.50 m on average) in elevation above pmsl. These surfaces are locally overflooded by the ground water table at maximum levels of 0.25 m (excavations C, D and F) (Fig. 11b, c, d). Analysis of the excavation walls reveal that the conglomerate-overlying, loose deposits increase noticeably in thickness and volume from Aramu to Vainono settings (Figs. 8, 9), probably in response to exposure to higher intensity and frequency of islet-building wave surges. The ocean-facing sequences (A and D) located just behind both the outer shingle ridges are 2.00 and 2.50 m thick at Motu Aramu and Motu Vainono respectively. In the middle parts of the islets, the thicknesses of the sedimentary sequences (B and E) are 0.90 and 2.00 m respectively. The sequences from the lagoon sides (C and F) are 1.10 and 2.10 m thick respectively.

The sequences consist usually of beds ranging from 0.20 to 0.60 m thick (Figs. 8, 9). However, locally, on Motu Vainono, single bed thickess can reach 1 to 2 m. Sediment grain-size decreases significantly from the ocean-facing shingle ridges (Fig. 11a, c) lagoonwards (Fig. 11b, d). Boulder- to cobble-dominated deposits laterally grade into pebble-dominated,

403 then in sand-dominated facies. Sediment composition and texture are quite similar between
404 Aramu and Vainono sites. Longest axis of coral boulders ranges between 300–350 mm to up
405 to 100 mm with mean values of around 200 mm. Along the islet transects, boulders particles
406 are progressively replaced by cobbles and pebbles. Boulders and cobbles consist
407 predominently of entire pocilloporid and fragmented acroporid colonies, associated to
408 merulinids and a few poritids (Fig. 7). Pebbly detritus are mainly composed of fragmented
409 pocilloporids, acroporids and merulinids, and low content of molluscan shells and coralline
410 algae. Sand-sized grains are composed of large foraminifera, molluscan, coral and coralline
411 debris. Foraminifera tests are dominated by soritids.

412 On the basis of textural attributes, four sedimentary facies can be recognized.

413 4.3.1. Boulder-cobble-dominated facies
414 This facies tends to be restricted to islet areas close to the ocean sides. It is prevalent at the
415 most exposed site (Excavation D) on Motu Vainono where it represents about 70 % of the
416 volume deposited (Fig. 9). By contrast, on Motu Aramu, within the ocean-facing excavation
417 (A), boulders and cobbles do not exceed 25 % of volume (Fig. 8). Surprisingly, there is a
418 layer composed of the same percentage of cobbles in Excavation C, close to the lagoon side at
419 Motu Aramu.

420 4.3.2. Pebble-dominated facies
421 It is subdivided into two subfacies as differentiated by its clast-supported characteristics:
422 pebble-supported and sand-supported. Pebble detritus (about 50 mm to 5 mm in diameter) are
423 dominantly composed of diverse coral debris, together with a few molluscan shells and
424 coralline algae. Both facies are found throughout both excavated islets (Figs. 8, 9, 11 a, c).
425 However, volumes of pebble-sized material is noticeably higher in Motu Vainono than in

Motu Aramu. The pebble-supported subfacies is the main component in the central part of Vainono islet (Excavation E) in which it occupies up to 60 % of the total volume while, in the central part of Aramu islet (Excavation B), it accounts for 20–25 % only. The sand-supported subfacies was encountered in both facing-ocean excavations (A, D) in which it represents 20 % and about 60 % of the total volumes respectively.

4.3.3. Sand-dominated facies.

Sandy material, enriched in low amounts (less than 10 %) of fine pebbles, is deposited predominantly within the inner islet zones, from the central parts towards the lagoonal border, on both Motu Aramu and Motu Vainono (Fig.11b, d). Higher sand amounts were found on Motu Aramu, through Excavations B and C, in which it represents 70 % and 80 % of the total volumes respectively. At Motu Vainono, within Excavations E and F, sand-dominated sediments occupied 25 % and 28 % of the cavity.

4.3.4. Organic-rich facies

This facies defines the occurrence of brown- to black-coloured, root-bearing horizons at the top part of most excavated sequences, usually at the expense of both pebble- to sand-dominated facies (Fig.11b, d). It is present at all excavation tops, but best developed on Vainono sites. There, its thickness ranges from 0.20 to 0.50 m. At Aramu settings, organic-rich layers are 0.050 to 0.25 m thick.

As a summary, it appears that the thicknesses of the different facies and subfacies vary markedly from Motu Aramu to Motu Vainono and from excavation to excavation. As expected, coarser deposits dominate in areas facing the open ocean, while finer ones are rather located near the lagoon sides. No apparent sediment grading was observed in any sequence nor any bed.

449 *4.4. Islet accretion chronology*

450 All ages of the dated coral samples extracted from excavations range approximately within
451 the last 5,000 year-interval – from 5,042 ± 16 cal.yr (M61) to 42 ± 2 cal.yr (M65). However,
452 the age distributional patterns differ between the both islets (Fig. 10). On Motu Aramu, two
453 major phases of clast supply occurred (Fig. 12a), the earlier from about 5,000 to 4,000 cal.yr,
454 and the later from 2,000 cal.yr to the modern, separated by a two millennia-long non-
455 depositional episode or a least by a slowdown in clast supply. By contrast, on Motu Vainono,
456 earlier deposition would have initiated between 5,000 and 4,000 cal.yr (Fig. 12a). There, the
457 main accretional episode would have lasted approximately 2,000 years, between 4,000 and
458 2,000 cal.yr. Accretion then progressively decreased in intensity until the modern times.

459 Few sequences have an age-decreasing trend from base to top, consistent with stratigraphy.
460 Despite some age inversions, in Excavations A and B (Aramu, outermost and mid islet sites)
461 and F (Vainono, lagoon-margin site), the older samples tend to be deposited in the lower beds
462 while the younger ones to be found close to the land surface. Within Excavation A, ages range
463 from 4,512 ± 12 cal.yr (M63) – 5,042 ± 16 cal.yr (M61) at base to 545 ± 4 cal.yr (M55) –
464 51 ± 2 cal.yr (M53) at top. Within Excavation B, ages decrease from 4,363 ± 13 cal.yr (M51)
465 to 1,820 ± 8 cal.yr (M47) and 108 ± 3 cal.yr (M44). Within Excavation F, ages are
466 2,278 ± 9 cal.yr (M84) at base, around 1,300–900 cal.yr in the medium beds and 42 ± 2 cal.yr
467 (M65) at top. But, in most cases, the samples are found to have been reworked and mixed. As
468 a whole, ages in the sections from Motu Aramu are distributed within a wide range while
469 those from Motu Vainono are distributed narrowly. Excavations A: 5,042 ± 16 cal.yr (M61)
470 to 51 ± 2 cal.yr (M53); B: 4,191 ± 8cal. yr (M52) to 108 ± 3 cal.yr (M47); C:
471 4,644 ± 25 cal.yr (M30 bis) to 882 ± 5 cal.yr (M38); D: 4,026 ± 13 cal.yr (M89) to
472 2,885 ± 8 cal.yr (M85); E: 3,293 ± 24 cal.yr (M134); F: 2,449 ± 10 cal.yr (M82). The average

age difference between the dated clasts into each excavation can be estimated as follows (Figs. 8, 9, 10): 5,000 years in Excavation A; 4,000 years in B; 4,200 years in C; 1,100 years in D; 1,000 years in E; 1,500 years in F. With a volume at least twice that of Motu Aramu, Motu Vainono is interpreted to have developed continuously and more rapidly throughout the same time interval, from several distinct depositional episodes of 1,000 to 1,500 years in duration.

Clasts older than 2,000 to 4,000 years are present within all the sequences, from the outermost as well as from the innermost islet sites, but best stratigraphically organized and mostly concentrated within the outermost excavation (A, D) deposits. This strongly suggests that the earlier depocentres from which the islets have accreted laterally have settled close to the ocean side, just behind the modern coastline. At Aramu, analysis of the age clast distribution within Excavations A and B advocates for an earlier clast deposition at approximately 5,000 to 4,500 cal.yr. At Vainono, in the outermost islet sections (Excavations D and E), the reported oldest clast ages range from about 4,000 to 3,000 years, thus supporting the interpretation that initiation of the depocentres may have occurred about 1,000 year later, compared to Aramu sites.

Along the lagoon sides, at Motu Aramu, in Excavation C, a number of younger clasts, varying in age from 1,808 ± 8 (M26 bis) to 882 ± 5 cal.yr (M38), are mixed with significantly older coral detritus, dated at 4,742 ± 14 (M28) to 4,037 ± 15 cal.yr (M37). Such an age mixture is regarded as resulting from a severe reworking of about 4,000 yr-old deposits during a later accretional phase of lagoonal islet borders, from about 1,800 cal.yr and probably during the last century. Similarly, on Motu Vainono, in Excavation F (lagoon side), clasts aged 2,500 cal.yr, found at top, and are mixed with some dated 1,600 to 900 cal.yr located downhole. Accordingly, a reworking and resedimentation of the lagoon margins is

thought to have occurred presumably during the last century or earlier. Similarly, the ocean-facing shingle ridges from which superficially deposited clasts yield ages ranging from about 70 (M19), 300 (M162, M164), 1,200 (M166), 2,500 (M21, M22, M24) to 3,500 (M167) cal.yr, are relatively moving structures, occasionally suffering reshaping.

As a summary, Motu Aramu and Motu Vainono are believed to have started developing between 5,000 and 4,500 (Fig. 13) and between 4,000 and 3,000 cal.yr (Fig. 14) respectively, from depocentres settled close to the present coastline. The innermost islet areas, that have probably emplaced about 500 to 1,000 years later, have suffered intense disturbance and reworking, resulting in mixtures between older than 4,000 yr or than 1,500 yr clasts with some younger than 1,800 cal.yr or aged 1,600–900 cal.yr respectively.

4.5. Islet accretion rates

The rate of islet accretion is obviously dependent on the frequency and intensity of wave-surge events, serving as both constructional and erosional agents, which have impacted the atoll over time, but also on the recovery rates of coral communities in the different source zones. For example, the acroporid- and pocilloporid-dominated coral populations along the upper outer-reef zone, i.e. the main source of coral-clasts, are growing at rates of several tens of centimetres per year. Accordingly, these would be able to regenerate after 20 years in high-energy settings (Y. Chancerelle, CRIOBE, pers. com.) at rates significantly higher than the apparent recurrence period of islet building events averaging 50 to 100 years.

The accretion rates of atoll-rim islets and adjacent shingle ridges can be estimated based on U/Th dating. Vertical accretion rates at Aramu and Vainonono sites range at around 2–3 to 6 cm per century respectively. Lateral accretion rates from the depocentres oceanwards range between less than 1 m per century at Aramu and 2–2.5 m per century at Vainono.

Progradation towards the lagoon margins occurred at rates averaging 3–3.5 and 7–9 m per century at Aramu and Vainono respectively. Shingle ridges have prograded to the ocean at rates of 75–60 cm per century at Aramu and 200–250 cm per century at Vainono. These values clearly take into account erosional and reworking phases, given major depositional events are known to have occurred through instantaneous, high-intensity, low-frequency wave surges.

5. Discussion

5.1. Islet-accretion and sea-level change

In the Tuamotu, the sea-level course during the mid to late Holocene times is relatively well constrained based on dating of exposed coral heads, conglomerates and remnants of reef flats (Pirazzoli and Montaggioni, 1986, 1988a, b) and elevated micro-atolls (Hallmann et al., 2018, 2020), especially, in the Gambier islands (Pirazzoli and Montaggioni, 1987) (Fig. 12b). After a rapid postglacial rise (Bard et al., 1996), sea level reached and outpassed its present position by approximately 6,000 cal.yr. Sea level continued to rise up irregularly to heights of about + 1m relative to pmsl, from 5,000 to 4,100 cal.yr, then remained stable over a period of about 600 years. From about 3,400 yr BP, sea level started to fall progressively (Hallmann et al., 2020). Between 3,000 and 1,500 cal.yr, sea level dropped step by step eaching its modern position during the last millennium (Pirazzoli and Montaggioni, 1987, 1986, 1988a, b; Hallmann et al., 2018, 2020).

Throughout the tropics, the initiation and building of atoll-rim islets would have taken place under different eustatic regimes: during a post-highstand sea-level fall (Woodroffe et al., 1999; Dickinson, 2009; Kench et al., 2014a, b; Yasukochi et al., 2014), a rise in sea level (Montaggioni et al., 2022) or stillstands higher than the present (McLean et al., 1978; Stoddart

et al., 1978; Woodroffe and Morrison, 2001; Kench et al., 2014a, b, 2020; Yamano et al., 2014). For example, in the north-west Tuamotu, on Takapoto Atoll, motu would have developed during the sea-level drop phase from 2,500 yr BP to present (Montaggioni et al., 2018, 2019). However, there is no evidence that the position of sea level during its course has played a significant role in atoll-islet building.

5.2. Timing and mode of islet-accretion

Radiometric dating of both islet foundations, i.e. conglomerate platforms, and overlying unconsolidated islet deposits, reveal that all these features have deposited over the last 5,000 years, from the mid to late Holocene (Figs. 10, 12a). These findings clearly indicate that the emplacement of Motu Aramu and Motu Vainono and their conglomerate foundations has taken place throughout the whole mid-late Holocene sea-level cycle. Atoll-rim nourishment by coral detritus on Aramu sites would have begun from about 5,000 cal.yr as sea-level was rising. Since the top surfaces of conglomerate platforms reach locally elevations of up to 1.00 m, it is obvious that their present-day position cannot be related to any higher sea stillstand during the mid-late Holocene (Montaggioni et al., 2021). The timing of deposition of rubble sheets from which conglomerates have formed is consistent with previous data gained from a number of other French Polynesian islands. These revealed that deposition of conglomerates has mostly taken place between 6,000 cal.yr to present, peaking between 4,000 and 1,000 cal.yr. It is instructive to recall that both deposition and consolidation of conglomeratic material and accretion of overlying atoll-rim islets were demonstrated to have occurred locally simultaneously. In other words, there have been interplays between deposition of antecedent rubble sheets behind conglomerate pavements and islet building (Montaggioni et al., 2021), as currently observed on Motu Tekava (Fig. 15).

566 The mode of islet development was identical on both Aramu and Vainono sites as illustrated
567 by isochron distribution (Figs. 13, 14). Islet accretion has been initiated from nodal points, i.e.
568 depocentres, as previously observed on Takapoto Atoll, north-west Tuamotu (Montaggioni et
569 al., 2019). However, there is no direct evidence that all islets present around the atoll rim have
570 accreted similarly, from prograding and final coalescence of a series of nearby isolated
571 depocentres, especially, in rim areas on which rest continuous, elongated islets, spreading
572 over several kilometres, as observed in the north-east rim. However, based on the present-day
573 physiography of the south-west rim, typified by alternations of small, isolated motu separated
574 by a series of functioning hoa, the accretional islet model involving prograding depocentres is
575 thought to be realistic (Fig. 16).

576 Starting at around 5,000 cal.yr, the first islet accretional event ended 4,000 yr ago at Aramu
577 sites (Fig. 12a). At the same time, islet deposition was initiated on Vainono reef-rim while sea
578 level peaked at +1m above pmsl (Fig. 12b). At Aramu, the postulated non-depositional
579 episode between 4,000 and 1,800 cal.yr, occurred during the about 600 yr-long high stillstand
580 and lasted up to one millennium. The second and final accretional event took place during the
581 last 1,800 years as sea level dropped to its modern position. Correlatively, over the last 4,000
582 years, at Vainono sites, coral clasts were supplied continuously (Fig. 12a), during both the
583 high sea stand and the following drop (Fig. 12b). Strong discrepancies in accretional histories
584 between two nearby islets from a same atoll clearly support the fact that sea-level dynamics is
585 not the major driver of atoll islet building in French Polynesia, contrary to some previous
586 interpretations in other reef provinces (Perry et al., 2011; Kench et al., 2014b, 2020), even if
587 there is apparently a close correspondence between the course of sea level and islet
588 nourishment by coral detritus on Motu Vainono. In fact, atoll-islet building seems to have
589 been no longer dependent on sea-level dynamics. Fluctuations of some tens of centimetres

590 have not been able to significantly influence the depositional islet patterns in regions
591 periodically subjected to storm wave surges. During the last 6,000 years, the only required
592 control of sea-level was the maintenance of a position close to present throughout the
593 complete cycle of islet accretion, thus facilitating supply of coral detritus from adjacent
594 forereef zones. However, it is noteworthy that initiation of islet accretion can operate even
595 when sea-level was several tens of metres below its present position during the postglacial
596 rising sea-level course, as observed on Rangiroa Atoll, northwestern Tuamotu. In such a case,
597 rubble deposition was interpreted as resulting from occasional tsunamis (Montaggioni et al.,
598 2022).

599 *5.3. Islet accretion: the key role of marine hazard events*

600 Natural hazards, including winter storms, cyclones, distant-source swells, tropical low waves
601 and tsunamis, are known to be drivers of formation and shaping of low-lying reef islands
602 (Woodroffe, 2008; Canavesio, 2019; Montaggioni, 2018, 2019 and references herein; Duvat
603 et al., 2020). Especially, most of them are able to move gravels and large boulders from
604 adjacent reef sources across atoll rims. Unfortunately, it is not possible to identify the
605 respective role of these different islet-building agents in the sedimentary record, especially
606 beyond the historical period due to the lack of record. Only assumptions can be made, based
607 on the frequency of each agent. In the Tuamotu, tropical lows and tsunamis usually produce
608 low intensity impacts, unlikely to be recorded in the sedimentary archives. Only the end-
609 products of tropical cyclones and extreme distant-source events are most likely to be
610 encapsulated into islet-sequences. The end-products are the result of both constructional and
611 erosional processes. The morphological and stratigraphical attributes of these products, i.e.
612 islets and associated shingle ridges and sheets, can provide valuable information on past

613 regional storm dynamics, i.e. frequency and intensity of wave surges impacting islands (Nott,
614 2011; Montaggioni, 2018, 2019).

615 At reef settings and, particularly, in French Polynesia, coral clasts and finer skeletal grains
616 deposited onto reef rims are known to have originated dominantly from the adjacent upper
617 forereef zones, mostly extracted from coral communities living at depths less than 25 m
618 (Laboute, 1985; Harmelin-Vivien and Laboute, 1986; Harmelin-Vivien, 1994) and partly
619 from coral communities living in outer reef-flat and lagoonal environments (Adjas, 1988), as
620 shown from taxonomic analysis of coral clasts and composition of groove sand pockets and
621 lagoonal deposits.

622 In the tropical Pacific, biogeochemical records and climate modelling indicated that mid
623 Holocene was a time of reduced ENSO variability (Clement et al., 2000; Koutavas et al., 2006;
624 Zhang et al., 2014; Emile-Geay et al., 2016; Lawman et al., 2020). Decreased ENSO frequency
625 took place at times in the last few thousand years (Emile-Geay et al., 2015). Cyclone-related
626 rainfall intensity increases after 4,200 yr BP, as well as at 3,200 and 2,000 yr BP in South
627 America (Conroy et al., 2008; Emile-Geay et al., 2015). In the Tuamotu, occurrences of
628 extreme marine wave hazards prior to the mid-nineteenth century are poorly documented
629 (Laurent and Varney, 2014). A comprehensive survey of extreme hydrodynamic events, based
630 on radiometric dating of mega-boulders was published by Lau et al., (2016), focusing only on
631 the central Tuamotu region. Boulder age suggested that 5–9 extreme marine events occurred
632 between 1200 and 1900 AD, with 3–5 events over the seventeenth and nineteenth centuries.
633 In the absence of mega-boulders on South-Marutea, using the U/Th clast-age database
634 provided herein can contribute to define the number of significant wave-surge events that
635 have struck the south-eastern Tuamotu end over the last 5,000 years. A total of 86 are
636 identified during this time span (Fig. 17), taking into account possible age overlapping

637 between samples as recognized from U/Th error range. The number of events recorded per
638 century ranges from zero to 5. It is evident that a database including a relatively limited
639 number of dated specimens cannot provide a comprehensive record of past hazard events.
640 Sedimentary sequences are well known to be truncated records of the depositional history of a
641 given environment (Sadler, 1999). Especially, traces of marine hydrodynamic events are
642 frequently poorly or incompletely preserved in atoll-rim ridge and beach stratigraphies. In
643 addition, defining the number of storm events recorded by any islet sequence may be biased
644 by sampling procedures including incomplete age determination (Nott, 2011). However,
645 assuming that an average of 1 to 5 cyclonic events per century with a mean recurrence time of
646 50 years is consistent with previous historical estimates (Dupon, 1987; Laurent and Varney,
647 2014; Lau et al., 2016), our data is thought to preserve a reliable picture of marine wave-surge
648 event history in the remote south-eastern Tuamotu at a centennial to millennial-scale
649 frequency over the last five millennia (Fig. 17). The historical period, i.e. the last two
650 centuries, includes 6 hazard events, respectively occurring in around 1817, 1914, 1949, 1971,
651 1975, and 1980. The last two younger samples (M138, M65) were probably projected onto
652 the atoll rim during the passage of cyclone Frances (February 1976) and cyclone Nano
653 (January 1983). Related to the year 1971 (M53), there is no direct record of a marine hazard
654 event within the Gambier region; the only record is that of a moderate tropical depression
655 (Vivienne) passed close through the Austral Archipelago, far from the Gambier. Similarly,
656 there is no evidence of a noticeable cyclone activity from 1914 (M44) to 1949 (M19) within
657 the entire Tuamotu region. As for the nineteenth century, only one sample (M18: 1817 ± 3
658 AD) accounts for a storm event at South-Marutea, but not validated in the historical registry.
659 It is noteworthy, as shown by Duvat et al. (2020), projection of coral clasts from outer reef
660 slopes to adjacent atoll rims can occur during tropical lows, under moderate hydrodynamical
661 conditions, without the involvement of any extreme hazard event. Such relatively low-wave

energy events do not get enough attention to be listed as part of significantly human-impacting climate phenomena.

Throughout pre-European historical times, from the beginning of the Common Era to the eighteenth century, clast dating allows a total of 35 hazard events distributed into three main periods of active storminess to be identified (Fig. 17): from the 18th to 15th, from the 12th to the 7th and from the 3rd to the 2nd centuries, apparently separated by two quiescent intervals between the 12th–15th and the 7th–3rd centuries respectively. Each active interval appears to have been separated from the next by a non-deposition interlude longer than 200 years, although this last event may also have incorporated islet-damaging phases.

The regional pattern successively shows a continuous, higher storm activity from about the 7th to the 12th centuries, broadly encompassing the Medieval Warm Period, followed by a brief decrease in storminess prior to the 15th century, and finally by a recovery of storm activity over a period (15th–19th centuries) apparently coinciding with the Little Ice Age. This pattern is regarded as consistent with reconstructed variability of past cyclone dynamics across the central south Pacific, controlled by a large shift of the Pacific Walker circulation (Bramante et al., 2020). Similarly, weakening of storminess over earlier, brief intervals within the Common Era could be caused by repeated migrations of the Walker circulation, thus mitigating the activity of ENSO events.

Throughout the three millennia-long period preceding the Common Era, 51 hazard occurrences are recorded, with a frequency of one to five per century (Fig. 17) as numerous as those observed during the 2,000 yr-long Common Era. However, the most striking feature is the absence of coral clast samples aged less than 4,000 cal.yr and more than 2,000 years old, collected at Aramu sites, while present in large numbers (17 counted samples) on Motu

Vainono (Fig. 12a). Several alternative explanations could be put forward. The absence of the relevant samples could be due to an artefact of collection or to suppression of the 4,000–2,000 yr time-specific coral-clast stocks due to intensive marine erosional phase. Another explanation could be found in the location of Motu Aramu, north of the atoll rim, likely to be less exposed to some extreme marine hazard events, such as distant-source wave surges, that come from the deep South Pacific, when compared to Vainono sites. Interestingly, the non-depositional episode at Aramu sites coincides with intervals of a relatively low-baseline cyclogenesis activity (Fig. 12c, d) and more sustained south-east trade winds in connection with an attenuation of ENSO amplitude by about 20 % to up to 60 % within the 5,000- to 2,000-yr band. This decrease in ENSO activity was documented by a number of sedimentary data collected from the central and eastern Pacific: foraminiferal records in the eastern Pacific basinal sediments (Koutouvas et a., 2006), coral archives from Line Islands in the central tropical Pacific (McGregor et al., 2013; Grothe et al., 2019), grain-size analysis of a sedimentary core from Junco Crater Lake in Galapagos (Conroy et al., 2008) and sediment laminae light-intensity in a core from Laguna Pallcacocha in Ecuador (Moy et al., 2002). Assuming that cyclogenesis was at its lowest level during this time span, deposition of high coral-clast volumes at north-facing Aramu sites may be caused by other marine hazards, including trade-wind-generated winter storms. By contrast, at south-facing Vainono sites, islet deposits emplaced during the 5,000–2,000 yr-interval may have been supplied by distant-source, austral swells.

As a summary, the age database provided herein seems to reliably reflect the variability of ENSO frequency events at centennial- to millennial scales through the number of recorded wave-surge events in the south-eastern Tuamotu end.

5.4. Conceptual model of atoll-rim islet building

A number of atoll-islet building models have been already described from some cyclone-prone or not-prone reef settings, based on reconstruction of low-lying, reef-rim and lagoon-islet development history, in the Indian and Pacific oceans. (Stoddart et al., 1978; Chivas et al., 1986; Richmond, 1992; McLean and Woodroffe, 1994; Woodroffe et al., 1999; Kench et al., 2005, 2012, 2014a, b, 2020; Barry et al., 2007; Yamano et al., 2014; Montaggioni et al., 2018, 2019; Liang et al., 2022). The initial baseline conditions required for optimal islet building and sustainability were defined as follows: (1) hard antecedent substrates, such as reef flats, conglomerate platforms, are usually prerequisite for islet settlement; (2) substrates have to be close or at sea level at the time of islet initiation; (3) maintenance of growing islets within the range of the sea-level course; (4) availability of sediment producers at close proximity; (5) recurrence of marine, high to low-intensity hazard events.

At South-Marutea, on both Motu Aramu and Motu Vainono, islet development occurred over the last 5,000 years while sea level followed a complete trajectory from rising to about +1 m to falling close to its present position (Fig. 12b). Conglomerate platforms, locally as high as +1.10 m relative to pmsl, started to form at around 5,000 cal.yr (Figs. 13, 14) during the rise in sea level. The widespread conglomerate deposits, locally consisting of one single bed, gives evidence of the occurrence of high-intensity, wave-surge events at a starting time of reduced ENSO activity in the central south Pacific. This strongly suggests that non-cyclonic events could occasionally play a dominant role in atoll-islet shaping. Contrary to Takapoto Atoll, northern Tuamotu, on which depocentres were initiated at the middle parts of the atoll-reef rims (Montaggioni et al., 2019), on South-Makatea, incipient depocentres settled over conglomerate pavements close to the outer atoll reef-rim margins, just behind the modern reef-flat zones (Fig. 16). Depocentres as originally preferential sites of clast deposition

formed isolated, probably subcircular to elongated features as similar in shape to smaller islets at present found along the south-western atoll rim (Fig. 1b). From 4,000 cal.yr, the depocentres have prograded seawards and lagoonwards at rates of several metres per century. It is noteworthy that conglomerate platforms and islets were continuously being formed until the present. At Aramu, the islet landscape was shaped in two stages, between 5,000 and 4,000 cal.yr and 2,000 cal.yr to present. At Vainono, the major shaping phases occurred from 4,000 to 3,000 cal.yr during the higher sea stillstand. By contrast, at Motu Aramu, the earlier development episode lasted throughout the rising sea-level phase, but development restarted only at the time while sea level was falling. This means that the position of sea level was not a major determinant of islet building. Islet nourishment took place at sea-level trajectory. In particular, the present findings show that gradual sea-level drop is not a general promoter of islet accretion, as pointed out by Dickinson (2004). The key controls of islet development, at least in the studied sites, appear to be changes in intensity and frequency of marine hazard events rather than sea-level fluctuations over time.

The islet accretionary model obtained from South-Marutea Atoll typically refers to the 'regular lagooward accretion' model described by Woodroffe et al. (1999) in which accretion begins from depocentres located close to oceanwards shore and then incrementally extends preferentially lagoonwards through time. This model differs markedly from that established at Takapoto, confirming that islet shaping patterns are complex and can vary signicantly from site to site.

5.5. Projected future climate regime and its effects in the south-eastern Tuamotu atoll region

In the last decades, warming peak during several ENSO occurrences has moved from the eastern to central Pacific on 100° longitude, accompanied by an increasing amplitude and decadal variability of ENSO events and strengthening of trade winds (Freund et al., 2019;

Grothe et al., 2019). Currently, anthropogenic forcings are postulated to affect global climate, especially in the Pacific tropics, altering the geographical distribution, frequency and intensity of storms (Cai et al., 2021) and strengthening trade-winds (Collins et al., 2010). Storminess, including cyclogenesis, would potentially be increased in the central Pacific, with rising sea surface temperatures and weakening of vertical wind shear predicted for the end of the 21st century (Bramante et al., 2020). For the late 20th century, climate observations and reconstructions revealed a significant increase in the central Pacific ENSO activity, at a rate of 2.5 to 9 events per 20 years. Similarly, in response to increased intensity of the ENSO regime in the next decades, cyclones are expected to become more frequent (about 20–40 %) during El Niño phases, but significantly less frequent during La Niña episodes (Chand et al., 2017).

Cyclones, known as one of the major causes of coral decline around the world (Harmelin-Vivien, 1994; De'ath et al., 2012), are expected to become potentially more destructive with ocean warming (Dixon et al., 2022). Knutson et al. (2020) reviewed knowledge regarding model predictions of global cyclone activity in response to human-induced warming. At 2 °C warmer than the pre-industrial times, global cyclogenesis will become more intense. In the central South Pacific, ENSO events tend to move the mean cyclone genesis loci eastwards, potentially resulting in cyclone influence in French Polynesia (Bramante et al., 2020). South poleward migration 1° latitude (about 100 km) per decade (Kossin et al., 2014; Studholme et al., 2022) may increase cyclone frequency in the remote south-eastern Tuamotu region. However, with the projected expansion of the tropical climate zone, there will have a potential reduction of cyclone activity (Bramante et al., 2020).

Large waves generated by storms and cyclones and wave amplification are significant hazards in the tropical Pacific. The largest extreme wave heights are active within the latitudinal 15°–25° south band. Model predictions indicated that the doubling of extreme El Niño frequency

780 in the next decades would have drastic effects on wave climate, particularly when combined
781 with sea-level rise (Stephen and Ramsay, 2014). Median extreme wave heights across the
782 entire south Pacific range from 7 to 11 m (Stephen and Ramsay, 2014) and, more specifically,
783 in French Polynesia (Canavesio, 2014).

784 Unfortunately, there is no available region-specific model projections of the cyclone behavior
785 in French Polynesia for the mid to late 21st century. However, some general trends, in part
786 speculative, emerge, based on climate models from the south-western Pacific (Knutson et al.,
787 2020) that could be applied to French Polynesia. Frequency of severe category 4 and 5 and
788 lower category cyclone as well could decrease by about 15–20 %. Average cyclone intensity
789 is expected to increase 2 %, at medium-to-high confidence levels. The resilience of coral reefs
790 would be more severely threatened by increasing cyclone intensity. However, wave surges,
791 generated by cyclones or other extreme marine hazard events, are known to impact patchily
792 coral reefs (Done, 1992; Harmelin-Vivien, 1994; Cheal et al., 2002, 2017). This may result in
793 preservation of undamaged coral-colonized zones from which abundance of coral
794 communities can recover, usually 10–20 years after impacts (Hamelin-Vivien, 1994; Halford
795 et al., 2004). In a number of locations, coral populations need particularly long periods for
796 recovery after an extreme cyclone damage. In the Tuamotu, recovery of coral communities is
797 estimated to average about 70 years (Cheal et al., 2017).

798 Sea-level rise projections suggest that globally the rise would be around 0.50 m under
799 optimistic scenarios and outpass 1.30 m under pessimistic ones (Horton et al., 2020). These
800 predictions are in line with expectations of sea-level rise in the Tuamotu, where the rise in sea
801 level would be about 0.80 to 1 m higher relative to 2010 at the end of the 21st century
802 (Botella, 2015). Accordingly, sea-level rise will result in higher storm flooding levels, but

probably will play a subordinate role compared to marine hazards able to generate swells as high as 12 m (Dalmalian et al., 2014).

Other disturbances to which coral reefs are exposed will be amplified (Cheal et al., 2017): loss of coral calcification potential (D'Olivio et al., 2019; Cornwall et al., 2021) due to increasing ocean acidification in relation to higher atmospheric CO_2 content; increasing sea surface temperatures; especially long duration (several months) of marine heat waves (Holbrook et al., 2019), some resulting in more coral bleaching and mortality episodes as those recorded during 1982–1983 (Hoegh-Gulberg and Salvat 1995), 1997–1998 (Mumby et al., 2001), and 2015–2016 in French Polynesia (Hédouin et al., 2020). Interacting effects of various disturbances may exacerbate lethal impacts and will increase the vulnerability of coral reefs to long-term degradation. All these will alter the capacity of coral communities to grow and thus diminish coral cover.

As a summary, in the south-eastern Tuamotu end, potential future change in extreme ENSO events may have profound impacts on atoll islet maintenance. Projected global increases in ENSO strength, cyclone intensity, sea level, combined with pH drop and decrease in coral recovery rate, will act to further enhance the impacts of future storm wave surge risk. Based on the review by Knutson et al. (2020), it appears obvious that the combined effects of rapid sea-level rise and increased cyclone activity will result in higher average storm inundation levels, assuming all other factors equal. Cyclone-generated inundation events would be less frequent, about a maximum of 1–2 per century, maybe less, but more destructive. Regarding the other marine hazard events, there is no specific available information about their behaviour over the next decades. Global warming will lead to strengthening of trade winds in the Pacific (Li et al., 2019) and of austral, distant-source swells. Under pessimistic sea-level rise scenarios, the inundated areas by distant swell surges would increase by up to 90 % by

827 2100, as modelled in Fiji (Wandress et al., 2020). Given different locations will likely respond
828 differentially, according to exposure to the arrival direction of marine hazards (Damlamian et
829 al., 2013), there is a need for assessment of site-specific impacts. On South-Marutea Atoll, the
830 present findings show that the north-eastern and south-eastern reef-rim sectors may be most
831 susceptible to be impacted and to suffer damage than the other areas. However, it is difficult
832 to assess the carbonate budget of atoll islets, increase or decrease, in response to climate
833 change.

834 *5.6. Lessons from the past.*

835 How may reconstructing the accretional mode of atoll-islets aid to illuminate their future
836 behaviour in the face of changing climate? First, the atoll-islet development at South-Marutea
837 occurred over the past 5,000 years, irrespective of sea-level position, as sea level rose about 1
838 m from 5,000 to 3,500 cal.yr then dropped close to its present position from 3,500 cal.yr to
839 the last centuries. This suggests that sea level was neutral, did not and will not play a
840 significant role in restricting or promoting islet accretion. If correct, if sea level will rise to up
841 to 1 m at the end of the 21st century, the position of sea level will not contribute to the
842 maintenance or destruction of atoll islets in the region considered. Second, according to
843 observations over the past millennia and historical records, future ENSO variability will
844 promote increasing cyclone activity, with stronger category cyclones, but their frequency will
845 be similar to the recent past, not exceeding 1 to 5 per century. Similarly, as emphasized by
846 Lau et al. (2016), if sea surface temperatures will increase through the current century as
847 projected by IPCC, higher temperatures will be favourable to increasing cyclogenesis and
848 storminess in the central South Pacific. However, the way in which atoll islets will respond in
849 the future is difficult to be clearly appreciated to uncertainties in the effects of cyclone impact.
850 A same cyclone is known to both contribute to building and destruction of low-lying reef

islets from a same atoll according to changing trajectories (Scoffin, 1993; Etienne, 2012). Probably, such as during the last millennia, the final budget will be accretional even if flooding episodes will be more frequent in response to increasing cyclone activity. The actual unknown comes from how reefal coral communities as sources of coral clasts will react to increases in water temperatures and ocean acidification. Any drop in coral cover and any shift to non-constructional communities will disturb or preclude coral-clast inputs to islets. As previously suggested (Montaggioni et al., 2021), it is noteworthy that conglomerate platforms, particularly in areas where these exceed 1 m in elevation, may contribute to the persistence of low-lying islets.

6. Conclusions

Several points arise from the chronostratigraphical analysis of rim islets from South-Marutea Atoll.

Islet lithostratigraphy is characterized by alternations of unorganized, mixed coral boulder to pebble and skeletal sand beds. Coarser-grained deposits consist dominantly of individual acroporid and pocilloporid colonies, together with subordinate merulinid and poritid detritus as known to house the adjacent forereef zones. Sand-grained sediments are mixtures of various reef-dwelling carbonate producers, especially, larger soritid foraminifera. As supported by substantial clast age inversion and local interbedding of cobbles and pebbles, substantial sediment reworking and redeposition took place at lagoonside settings, hence expressing occasional intense wave agitation of lagoonal waters.

Contrary to Takapoto atoll islets in the north-western Tuamotu, emplaced during the last 2,500 years as sea level was falling (Montaggioni et al., 2019), islet initiation at South-Makatea sites occurred from about 5,000 cal.yr. Islet development apparently occurred

874 independently of the mid to late Holocene sea-level course. In northern sectors, islet accretion
875 slowed down significantly from 4,000 to 2,000 cal.yr, likely in response to weakening El
876 Niño activity. By contrast, in reef-rim areas oriented to due south, islet building acted
877 continuously and even peaked in the 4,000–2,000 cal.yr interval, may be in response to
878 increasing storminess from the deep south regions. Between 5,000 and 3,000 cal.yr, islet
879 accretion responded contrastingly at the local scales, very active on the southern atoll-rim and
880 ineffective in the northern areas. Availability rate of coral-dominated sediment stocks and
881 frequency and intensity of marine hazard events are regarded as the key factors for islet
882 building.

883 The clast-age distributional pattern suggests that, over the last 5,000 years, high-energy wave
884 events occurred at frequency of one to five per century, in accordance with the historical
885 records in French Polynesia, occasionally interrupted by 200 to 300 yr-long quiescence times.
886 The outer shingle ridges may have been reshaped during the last millennium, at least ten
887 times, based on clast dating.

888 The evolution of atoll-rim islets on South-Marutea in the future is difficult to predict, mainly,
889 because model climate projections are missing in the considered region. In the next few
890 decades, based on non-deposition of mega-boulders on the atoll over the last centuries, it is
891 unlikely that extreme marine hazard events will impact the atoll. Later, as the zone of cyclone
892 influence is moving polewards and cyclone intensity is increasing, but frequency decreasing,
893 South-Marutea and the nearby Gambier Island Group could possibly be impacted by stronger,
894 but fewer cyclones prior to the end of the 21st century Of course, actual damaging effects on
895 islets would depend upon the arrival direction and heights of generated wave surges and, as
896 recently, the southern rim sectors would risk to be most disturbed than other. A future sea
897 level at about +1m relative to present would not increase the disturbing effects of storms

predicted to generate waves of up to 10 m high. Assuming a return time of 50 to 100 years for stronger storm events and a predicted coral recovery time averaging 70 years, the potential detritus stocks used to rebuild islets may be reduced drastically over a few centuries. Up to 1 m high, conglomerate platforms could serve as natural flood defense and thus contribute to islet durability.

Acknowledgements

This work was partly supported by the POLYCONE (Integrated and Sustainable Regulation of Cones in Eastern Polynesia) research project. Field work was conducted from 20th November to 26th November 2021, by BS, GP and JMZ. BS conceived the original project, through discussions and exchanges with LFM. U/Th datations were performed by EPB. LFM, the corresponding author, was in charge of interpretating all the collected data and of writing the manuscript. He leads the manuscript development, in collaboration with all co-authors. BS and GP provided field pictures. Figures were conceived by LFM and BM-G and drawn by BM-G.

The authors warmly thank the following colleagues for their contribution, particularly, Tamatoa Bambridge, coordinator of POLYCONE at the French Polynesian level. Field work has benefited from logistical and financial support and help by Robert Wan, the owner of South-Marutea Atoll, Johnny-John R. Atger-Wan, his atoll manager. The atoll team members, Mike Tahai and Claudio Temauri, are acknowledged for effective engineering of the excavations in Aramu and Vainono atoll sites. Many thanks to the anonymous reviewers whose comments have significantly helped improving an early version of the manuscript. The three anonymous reviewers and Editor-in-Chief Xinyu Wang are warmly thanked for their helpful criticism and suggestions for improvement.

Declaration of competing interest

The authors declate to have no competing interest.

References

Adjas, A., 1988. Sédimentologie comparée de quelques modèles lagonaires actuels des milieux récifaux coralliens du Pacifique (Nouvelle Calédonie, Polynésie). PhD Thesis. Aix-Marseille Univ., p. 340.

Amores, A., Marcos, M., Le Cozannet, G., Hinkel, J., 2022. Coastal flooding and mean sea- level rise allowances in atoll island. Science Reports 12, 1281.

Andrefoüet, S., Ardhuin, F., Queffeulou, P., Le Gendre, R., 2012. Island shadow effect and the wave climate of the Western Tuamotu Archipelago (French Polynesia) inferred from altimetry and numerical model data. Marine Pollution Bulletin 65, 415e424.

Bard, E., Hamelin, B., Arnold, M., Montaggioni, L.F., Cabioch, G., Faure, G., Rougerie, F., 1996. Deglacial sea-level record from Tahiti corals and the timing of global meltwater discharge. Nature 382, 241–244.

Barry, S.J., Cowell, P.J., Woodroffe, C.D., 2007. A morphodynamic model of reef-island de- velopment on atolls. Sedimentary Geology 197, 47–63.

Bjerknes, J., 1969.Atmospheric teleconnections from the equatorial Pacific.Monthly Weather Review 97, 163–172.

Biribo, N., Woodroffe, C.D., 2013. Historical area and shoreline change of reef islands around Tarawa Atoll, Kiribati. Sustainability Science 8, 345–362.

Botella, A., 2015. Past and future sea level changes in French Polynesia. University of Ottawa, Canada, MSc thesis, p. 94.

Bourrouilh-Le Jan, F.G., Talandier, J., 1985. Sédimentation et fracturation de haute énergie en milieu récifal: tsunamis, ouragans et cyclones et leurs effets sur la sédimentologie et la géomorphologie d'un atoll: motu et hoa, Rangiroa, Tuamotu, Pacifique SE. Marine Geology 67, 263–272.

Bramante, J.F., Ford, M.R., Kench, P.S., Ashton, A.D., Toomey, M.R., Sullivan, M.R., Karnauskas, K.B., Ummenhofer, C.C., Donnelly, J.P., 2020. Increased typhoon activity in the Pacific deep tropics driven by Little Ice Age circulation changes. Nature Geoscience 13, 806–811.

Cai, W., Santoso, A., Collins, M., Dewitte, B., et al., 2021. Changing El Niño-Southern Oscillation in a warming climate. Nature Reviews Earth & Environment 2, 628–644.

Canavesio, R., 2014. Estimer les houles cycloniques à partir d'observations météorologiques limitées : exemple de la submersion d'Anaa en 1906 aux Tuamotu (Polynésie Française). VertigO, 14, 1–18.

950 Canavesio, R., 2019. Distant swells and their impacts on atoll and tropical coastlines. The exemple pf submersions
951 produced by lagoon water filling and flushing currents in French Polynesia during 1996 and 2011 mega swells.
952 Global and Planetary Change 177, 116–126.

953 Chand, S.S., Tory, K.J., Ye, H., Walsh, K.J.E., 2017. Projected increase in El-Niño driven-tropical cyclone
954 frequency in the Pacific. Nature Climate Change 7, 123–127.

955 Cheal, A.J., Coleman, G., Delean, S., Miller I., Osborne, K., Sweatman, H., 2002. Responses of coral and fish
956 assemblages to a severe but short-lived tropical cyclone on the Great Barrier Reef, Australia. Coral Reefs 21, 131–
957 142.

958 Cheal, A.J., Macneil, M.A., Emslie, M.J., Sweatman, H., 2017. The threat to coral reefs from more intense
959 cyclones under climate change. Global Change Biology doi: 10.1111/gcb.13593

960 Cheng, H., Lawrence Edwards, R., Shen, C.-C., Polyak, V.J., Asmerom, Y., Woodhead, J.D., Hellstrom, J., Wang,
961 Y., Kong, X., Spötl, C., Wang, X., Calvin Alexander, E., 2013. Improvements in ^{230}Th dating, ^{230}Th and ^{234}U half-
962 life values, and U/Th isotopic measurements by multi-collector inductively coupled plasma mass spectrometry.
963 Earth Planetary Science Letters 371–372, 82–91.

964 Chivas, A., Chappell, J., Polach, H., Pillans, B., Flood, P., 1986. Radiocarbon evidence for the timing and rate of
965 island development, beach-rock formation and phosphatization at Lady Elliot Island, Queensland, Australia.
966 Marine Geology 69, 273–287.

967 Clement, A.C., Seager, R., Cane, M.A., 2000. Suppression of El Niño during the mid-Holocene by changes in the
968 Earth's orbit. Paleoceanography 15, 731–737.

969 Collins, M., An, S.-I., Cai, W., Ganachaud, A., Guilyardi, E., Jin, F.-F., Jochum, M., Lengaigne, M., Power, S.,
970 Timmermann, A., Vecchi, G., Witenberg, A., 2010. The impact of global warming on the tropical Pacific Ocean
971 and El Niño. Nature Geoscience 3, 391– 397.

972 Connell, J., 2013. Islands at risk? Environments, Economies and Contemporary Change. Edward Elgar Publishing,
973 Cheltenham, UK, p. 351.

974 Conroy, J.L., Overpeck, J.T., Cole, J.E., Shanahan, T.M., Steinitz-Kannan, M., 2008. Holocene changes in eastern
975 tropical Pacific climate inferred from a Galapagos lake sediment record. Quaternary Science Reviews 27, 1166–
976 1180.

977 Cornwall, C.E., Comeau, S., Kornder, N., Lowe, R. J., 2021. Global declines in coral reef calcium carbonate
978 production under ocean acidification and warming. PNAS, 118, e2015265118.

979 Costa, M. B., Macedo, E. C., Siegle, E., 2017. Planimetric and volumetric changes of reef islands in response to
980 wave conditions. Earth Surface Processes and Landforms 42, 2663–2678.

Damlamian, H., Kruger, J., Turagabeci, M., Kumar, S., 2013. Cyclone wave inundation models for Apataki, Arutua, Kauehi, Manihi and Rangiroa Atolls, French Polynesia. SPC Applied Geoscience and Technology Division (SOPAC) Technical report PR176.

De'ath, G., Fabricius, K.E., Sweatman, H., Puotinen, M., 2012. The 27-year decline of coral cover on the Great Barrier Reef and its causes. PNAS 109, 17995–17999.

Dickinson, W. R., 2009. Pacific atoll living: how long already and until when. GSA Today 19, 4.

Dixon, A. M., Puotinen, M., Ramsay, H. A., Beger, M., 2022. Coral reef exposure to damaging, tropical cyclone waves in a warming climate. Earth's Future 10, e2021EF002600.

D'Olivio, J.P., Ellwood, G., DeCarlo, Th.M., McCulloch, M.T., 2019. Deconvolving the long-term impacts of ocean acidification and warming on coral biomineralisation. Earth Planetary Science Letters 526, 115785.

Done, T.J., 1992. Effects of tropical cyclone waves on ecological and geomorphological structure.s of the Great Barrier Reef. Continental Shelf Research 12, 859–872.

Dupon, J.-F., 1987. Les atolls et le risque cyclonique : le cas de Tuamotu. Cahiers des Sciences Humaines 23, 567–599.

Dupuy, C., Vidal, Ph., Maury, R.C., Guille, G., 1993. Basalts from Mururoa, Fangataufa and Gambier islands (French Polynesia): Geochemical dependence on the age of the lithosphere. Earth and Planetary Science Letters 117, 89–100.

Duvat, V.K.E., 2019. A global assessment of atoll island planform changes over the Past decades. WIREs Climate Change 10, e557.

Duvat, V.K.E., Pillet, V., 2017. Shoreline changes in reef islands of the central Pacific: Takapoto Atoll, Northern Tuamotu, French Polynesia. Geomorphology 282, 96–118.

Duvat, V. K. E., Salvat, B., Salmon, C., 2017a. Drivers of shoreline change in French Pacific atoll reef islands. Global and Planetary Change, 158, 134–154.

Duvat, W.K.E., Magnan, A.K., Russell, R.M., Hay, J.E., Fazey, I., Hinkel, J., Stojanovic, T., Yamano,H., Ballu, V., 2017b. Trajectories of exposure and vulnerability of small islands to climate change. WIREs Climate Change, e478.

Duvat, V.K.E., Pillet, V., Volto, N., Terorotua, H., Laurent, V., 2020. Contribution of moderate climate events to atoll island building. Geomorphology 354, 107057.

Emile-Geay, J., Cobb, K.M., Carré, M., Braconnot, P., Leloup, J., Zhou, Y., Harrison, S.P., Corrège, T., McGregor,H.V., Collins, M., Driscoll, R., Elliot, M., Schneider, B., Tudhope, A., 2016. Links between tropical Pacific seasonal, interannual and orbital variability during the Holocene. Nature Geoscience 9, 168–173.

1012 Etienne, S., 2012. Marine inundation hazards in French Polynesia: geomorphic impacts of Tropical Cyclone Oli in
1013 February 2010. Geological Society, London, Special Publication 361, 21–39.

1014 Etienne, S., Buckley, M., Paris, R., Nandasena, A.K., Clark, K., Strotz, L., Chagué-Goff, C., Goff, J., Richmond,
1015 B., 2011. The use of boulders for characterising past tsunamis: lessons from the 2004 Indian Ocean and 2009
1016 South Pacific tsunamis. Earth-Science Reviews 107, 76–90.

1017 Ford, M., 2012. Shoreline changes on an urban atoll in the Central Pacific Ocean: Majuro Atoll, Marshall Islands.
1018 Journal of Coastal Research 28, 11–22.

1019 Ford, M., 2013. Shoreline changes interpreted from multi-temporal aerial photographs and high resolution satellite
1020 images: Wotje Atoll, Marshall Islands. Remote Sensing of Environment 135, 130–140.

1021 Ford, M. R., Kench, P. S., 2014. Formation and adjustment of typhoon-impacted reef islands interpreted from
1022 remote imagery: Nadikdik Atoll, Marshall Islands. Geomorphology, 214, 216–222.

1023 Ford, M.R., Kench, P.S., 2015. Multi-decadal shoreline changes in response to sea level rise in the Marshall
1024 Islands. Anthropocene 11, 14–24.

1025 Fox-Kemper, et al., 2021. Ocean, cryosphere and sea level change. In Climate Change 2021: The Physical Science
1026 Basis. Contribution of Working Group I to the Sixth Assessment Report of the Intergovernmental Panel on Climate
1027 Change [Masson-Delmotte, V., et al., Eds.]. Cambridge University Press, Cambridge, UK and New York, USA,
1028 1211–1362.

1029 Freund, M.B., Henley, B.J., Karoly, D.J., McGrgor, H.V., Abram, N.J., Dommenget, D., 2019. Higher frequency of
1030 central Pacific El Niño events in recent decades relative to past centuries. Nature Geoscience 12, 450–455.

1031 Grothe, P. R., Cobb, K. M., Liguori, G., Di Lorenzo, E., Capotondi, A., Lu, Y., et al., 2019. Enhanced El Niño-
1032 Southern Oscillation variability in recent decades. Geophysical Research Letters 46, e2019GL083906.

1033 Halford, A., Cheal, A.J., Ryan, D., Williams, D.M.C.B., 2004. Resilience to large-scale disturbance in coral and
1034 fish assemblages on the Great Barrier Reef. Ecology 85, 1892–1905.

1035 Hallmann, N., Camoin, G., Eisenhauer, A., Botella, A., Milne, G.A., Vella, C., Samankassou, E., Pothin, V.,
1036 Dussouillez, P., Fleury, J., Fietzke, J., 2018. Ice volume and climate changes from a 6000 year sea-level record in
1037 French Polynesia. Nature Communication 9, 285.

1038 Hallmann, N., Camoin, G., Eisenhauer, A., Samankassou, Vella C., Botella, A., Milne, G. A., Pothin, V.,
1039 Dussouillez, P., Fleury, G., Fietzke, J., Goepfert, G., 2020. Reef response to sea level and environmental changes
1040 in the Central South Pacific over the past 6000 years. Global and Planetary Change 195, 103357.

1041 Hameed, S.N., Dachao, J., Thilakan, V., 2018. A model for Super El Niños. Nature Communications 9: 2528,
1042 doi:10.1038/s41467-018-04803-7.

1043 Harmelin-Vivien, M.L., 1994. The effects of storms and cyclones on coral reefs: a review. Journal of Coastal
1044 Research Special Issue 12, 211e231.

1045 Harmelin-Vivien, M.L., Laboute, P., 1986. Catastrophic impact of hurricanes on atoll outer reef slopes in the
1046 Tuamotu (French Polynesia). Coral Reefs 5, 55–62.

1047 Hédouin, L., Rouzé, H., Berthe, C., Pérez-Rosales, G., Martinez, E., Chancerelle, Y., Galand, P.E., Lerouvreur, F.,
1048 Nugues, M.M., Pochon, X., Siu, G., Steneck, R., Planes, S., 2020. Contrasting patterns of mortality in Polynesian
1049 coral reefs following the third global coral bleaching event in 2016. Coral Reefs 39, 939–952.

1050 Heinrich, Ph., Guibourg, S., Roche, R., 1996. Numerical modeling of the 1960 Chilean Tsunami. Impact in French
1051 Polynesia. Physics and Chemistry of the Earth 21, 19–25.

1052 Hoegh-Guldberg, O., Salvat B. 1995. Periodic mass-bleaching and elevated sea temperatures: bleaching of outer
1053 reef slope communities in Moorea, French Polynesia. Marine Ecology Progress Series 121, 181–190.

1054 Hoeke, R. K., McInnes, K. L., Kruger, J. C., McNaught, R. J., Hunter, J. R., Smithers, S. G., 2013. Widespread
1055 inundation of Pacific islands triggered by distant-source wind-waves. Global Planetary Change 108, 128–138.

1056 Holbrook, N.J., Scannell, H.A., Gupta, A.S., Benthuysen, J.A., Feng, M., Oliver, E.C.J., Alexander, L.V.,
1057 Burrows, M.T., Donat, M.G., Hobday, A., J., Moore, P.A., Perkins-Kirkpatrick, S.A., Smale, D.A., Straub, S.C.,
1058 Vernberg, Th., 2019. Nature Communication 10, 2624.

1059 Horton, B.P., Khan, N.S., Cahill, N., Lee, J.S.H., Shaw, T.A., Garner, A.J., Kemp, A.C., Engelhart, S.E.,
1060 Rahmstorf, S., 2020. Estimating global mean sea-level rise and its uncertainties by 2100 and 2300 from an expert
1061 survey. Climate and Atmospheric Science 3, 18.

1062 Hubbard, D., Gischler, E., Davies, P., Montaggioni, L.F., Camoin, G., Dullo, C.W., Storlazzi, C., Field, M.,
1063 Fletcher, C., Grossman, E., Sheppard, C., Lescinsky, H., Fenner, D., McManus, J., Scheffers, S., 2014. Island
1064 outlook: warm and swampy. Science 345, 6203.

1065 Ito, G., McNutt, M., Gibson, R.L., 1995. Crustal structure of the Tuamotu Plateau, 15°S, and implications for its
1066 origin. Journal of Geophysical Research 100, 8097–8114.

1067 Jaffey, A.H., Flynn, K.F., Glendenin, L.E., Bentley, W.C., Essling, A.M., 1971. Precision measurements of half-
1068 lives and specific activities of ^{235}U and ^{238}U. Physical Review 4, 1889–1906.

1069 Kao, H.Y., Yu, J.Y., 2009. Contrasting eastern-Pacific and central-Pacific types of ENSO. Journal of Climate 22,
1070 615–632.

1071 Kench, P.S., 2014. Developments in coral reef and reef island geomorphology: editorial. Geomorphology 222, 1–2.

1072 Kench, P.S., McLean, R.F., Nichol, S.L., 2005. New model of reef-island evolution: Maldives, Indian Ocean.
1073 Geology 33, 145–148.

1074 Kench, P. S., Brander, R. W., 2006. Response of reef island shorelines to seasonal climate oscillations: South
1075 Maalhosmadulu atoll, Maldives. Journal of Geophysical Research 111, F01001. doi: 10.1029/2005JF000323

1076 Kench, P.S., Chan, J., Owen, S.D., McLean, R.F., 2014a. The geomorphology, development and temporal dynamics
1077 of Tepuka Island, Funafuti atoll, Tuvalu. Geomorphology 222, 46–58.

1078 Kench, P.S., Owen, S.D., Ford, M.R., 2014b. Evidence for coral island formation during rising sea level in the
1079 central Pacific Ocean. Geophysical Research Letters 41, 820–827.

1080 Kench, P.S., Owen, S.D., Beetham, E.P., Mann, Th., McLean, R.F., Ashton, A., 2020. Holocene sea level
1081 dynamics drive formation of a large atoll island in the central Indian Ocean. Global Planetary Change 195,
1082 103354.

1083 Knutson, Th., Camargo, S.J., Chan, J.C.L., Emanuel, K., Ho, Ch.-H., Kossin, J., Mohapatra, M., Satoh, M., Sugi,
1084 M., Walsh, K., Wu, L., 2020. Tropical cyclones and climate change assessment. Part II: projected response to
1085 anthropogenic warming. Bulletin of the American Meteorological Society. doi:10.1175/BAMS-D-18-0194.1

1086 Kopp, R.E., Simmons, F.J., Mitrovica, J.X., Maloof, A.C., Oppenheimer, M., 2009. Probablistic assessment of sea
1087 level during the last interglacial stage. Nature 462, 863–867.

1088 Kossin, J., Emanuel, K.A., Vecchi, G.A., 2014. The poleward migration of the location of tropical cyclone
1089 maximum intensity. Nature 509, 349–352.

1090 Koutavas, A., de Menocal, P.B., Olive, G.C., Lynch-Stieglitz, J., 2006. Mid-Holocene El Niño-Oscillation (ENSO)
1091 attenuation revealed by individual foraminifera in eastern tropical Pacific sediments. Geology 34, 993-996.

1092 Laboute, P., 1985. Evaluation des dégâts causés par les passages des cyclones de 1982–1983 en Polynésie
1093 Française sur les pentes externes des atolls de Tikehau et de Takapoto (Archipel des Tuamotu). Proceeding of the
1094 Fifth International Coral Reef Congress 3, 323–329.

1095 Larrue, S., Chiron, Th., 2010. Les îles de Polynésie Française face à l'aléa cyclonique. VertigO 10.
1096 https://doi.org/10.4000/vertigo.10558.

1097 Lau, A.Y.A., Terry, J.P., Switzer, A.D., Lee, Y., Etienne, S., 2016. Understanding the history of extreme wave
1098 events in the Tuamotu Archipelago of French Polynesia from large carbonate boulders on Makemo Atoll, with
1099 implications for future threats in the central South Pacific. Mar. Geol. 380, 174-190.

1100 Laurent, V., Varney, P., 2014. Histoire des cyclones de Polynésie Française de 1831 à 2010, ISBN 978-2-9522946-
1101 1-4, p. 172. Météo-France.

1102 Lawman, A.E., Di Nezio, P.N., Partin, J.W., Dee, S.G., Thirumalai, K., Quinn, T.M., 2022. Sciences Advances 8,
1103 eabm4313.

1104 Lecacheux S., Bulteau T., Pedreros R., Delvallée E., Paris F., 2013. Projet ARAI 3 : évaluation probabiliste des
1105 houles et des surcotes cycloniques en Polynésie Française. Rapport BRGM/RP-61888-FR, p. 122.

Le Cozannet, G., Garcin, M., Yates, M., Idier, D., Meyssignac, B., 2014. Approaches to eval- uate the recent impacts of sea-level rise on shoreline changes. Earth-Science Reviews 138, 47–60.

Li, Y., Chen, Q., Liu, X., Li, J., Xing, N., Xie, F., Feng, J., Zhou, X., Cai, H., Wang, Z., 2019. Long-term trend of the tropical Pacific trade winds under global warming and its causes. Journal of Geophysical Research: Oceans 124, 2626–2640.

Magnan, A.K., Ranché, M., Duvat, V.K.E., Prenveille, A., Rubia, F., 2018. L'exposition des populations des atolls de Rangiroa et de Tikehau (Polynésie française) au risque de submersion marine. VertigO 18, 1–35.

Magnan, A.K., Oppenheimer, M., Garschagen, M., Buchanan, M. K., Duvat, V. K. E., Forbes, D. L., Ford, J. D., Lambert, E., Petzold, J., Renaud, F. G., Sebesvari, Z., van de Wal, R. S. W., Hinkel, J., Pörtner, H-O., 2022. Sea level rise risks and societal adaptation benefits in low-lying coastal areas. Science Reports 12, 10677.

McGregor, H.V., Fischer, M.J., Gagan, M.K., Fink, D., Phipps, S.J., Wong, H., Woodroffe, C.D., 2013.A weak El Niño-Southern Oscillation with delayed seasonal growth around 4,300 years ago. Nature Geoscience 6, 949–953.

McLean, R. F., Stoddart, D. R., Hopley, D., Polach, 1978. Sea level change in the Holocene on the Northern Great Barrier Reef. Philosophical Transactions of the Royal Society of London A 291, 167–186.

McLean, R.F., Woodroffe, C.D., 1994. Coral atolls. In: Carter, R.W.G., Woodroffe, C.D. (Eds.), Coastal Evolution: Late Quaternary Shoreline Morphodynamics. Cambridge Univ. Press, Cambridge, United Kingdom, pp. 267–302.

McLean, R.F., Kench, P., 2015. Destruction or persistence of coral atoll islands in the face of 20th and 21st century sea-level rise? WIREs Climatic Change 6, 445–463.

Montaggioni, L.F., Salvat, B., Aubanel, A., Eisenhauer, A., Martin-Garin, B., 2018. The mode and timing of windward reef-island accretion in relation with Holocene sea- level change: a case study from Takapoto Atoll, French Polynesia. Geomorphology 318, 320–335.

Montaggioni, L.F., Salvat, B., Aubanel, A., Pons-Branch, E., Martin-Garin, B., Dapoigny, A., Goeldner-Gianella, L., 2019. New insights into the Holocene development history of a Pacific low-lying coral island: Takapoto Atoll, french Polynesia. Quaternary Science Reviews 223, 105947.

Montaggioni, L.F., Martin-Garin, B., Salvat, B., Aubanel, A., Pons-Branchu, E., Paterne, M., Richard, M., 2021. Coral conglomerate platforms as foundations for low-lying, reef islands in the French Polynesia: new insights into the timing and mode of formation. Marine Geology 437, 106500.

Montaggioni, L.F., Baltassat, J.-M., Le Cozannet, G., Innocent, Ch., Martin-Garin, B., Salvat, B., 2022. Reef-rim structure and building history, Rangiroa, an uplifted Atoll, French Polynesia: the role of morphotectonics and extreme marine hazard events. Marine Geology 445, 106748.

Mumby P, Chisholm J, Edwards A, Clark C, Roark E, Andrefouet S, Jaubert, J., 2001. Unprecedented bleaching-induced mortality in Porites spp. at Rangiroa atoll. French Polynesia. Marine Biology 139, 183–189.

Moy, Ch., M., Seltzer, G.O., Rodbell, D.T., Anderson, D.M., 2002. Variability of El Niño-Southern Oscillation activity at millennial timescales during the Holocene epoch. Nature 420, 162–165.

Müller, R. D., Roest, W. R., Royer, J-Y., Gahagan, L. M., Sclater, J. G., 1997. Digital isochrons of the world's ocean floor. Journal of Geophysical Research 102, 3211–3214.

Nott, J.F., 2011. Tropical cyclones, global climate change and the role of Quaternary studies. Journal of Quaternary Science 26, 468–473.

Pala, C., 2014. Warming may not swamp islands. Science 345, 496–497.

Pedreros, R., Krien, Y., Poisson, B., 2010. Programme ARAI 2. Caractérisation de la submersion marine liée aux houles cycloniques en Polynésie française. Rapport BRGM/RP- 58990-FR, 64 p.

Perry, C.T., Kench, P.S., Smithers, S.G., Riegl, B., Yamano, H., O'Leary, M.J., 2011. Implications of reef ecosystem change for the stability and maintenance of coral reef islands. Global Change Biology 17, 3679–3696.

Pirazzoli, P.A., Montaggioni, L.F., 1986. Late Holocene sea-level changes in the northwest Tuamotu Islands, French Polynesia. Quaternary Research 25, 350–368.

Pirazzoli, P.A., Montaggioni, L.F., 1987. Les îles Gambier et l'atoll de Temoe (Polynésie Française) : anciennes lignes de rivage et comportement géodynamique. Géodynamique 2, 13–25.

Pirazzoli, P.A., Montaggioni, L.F., 1988a. Late Holocene sea-level changes in French Polynesia. Palaeogeography, Palaeoclimatology, Palaeoecology 68, 153–175.

Pirazzoli, P.A., Montaggioni, L.F., Salvat, B., Faure, G., 1988b. Late Holocene sea level indicators from twelve atolls in the central and eastern Tuamotus (Pacific Ocean). Coral Reefs 7, 57–68.

Pons-Branchu, E., Douville, E., Dumont, E., Branchu, P., Thil, F., Frank, N., Bordier, L., Borst, W., 2014. Cross-dating (U/Th and lamina counting) of modern carbonate deposits in underground Paris, France. A new archive for urban history reconstructions: case study of anthropic Rare Earth and Yttrium release. Quaternary Geochronology 24, 44e53.

Pörtner, H.-O., Roberts, D.C., Tignor, M., Poloczanska, E.S., Mintenbeck, K., Alegría, A., Craig, M., Langsdorf, S., Löschke, S., Möller, V., Okem, A., B. Rama, R. (eds.), 2022. IPCC: climate change 2022: impacts, adaptation and vulnerability. Contribution of Working Group II to the Sixth Assessment Report of the Intergovernmental Panel on Climate Change Cambridge University Press. Cambridge University Press, Cambridge, UK and New York, NY, USA, 3056 pp. doi:10.1017/9781009325844.

Purkis, S. J., Gardiner, R., Johnston, M. W., Sheppard, C. R. C., 2016. A half-century of coastline change in Diego Garcia - the largest atoll island in the Chagos. Geomorphology 261, 282–298.

1169 Rankey, E. C., 2011. Nature and stability of atoll island shorelines: gilbert Island chain, Kiribati, equatorial
1170 Pacific: atoll shoreline change, equatorial Pacific. Sedimentology 58, 1831–1859.

1171 Reymond, D., Hyvernaud, O., Okal, E.A., 2013. The 2010 and 2011 tsunamis in French Polynesia: operational
1172 aspects and field surveys. Pure and Applied Geophysics 170, 1169–1187.

1173 Richmond, B.M., 1992. Development of atoll islets in the central Pacific. Proc. Seventh International Coral Reef
1174 Symposium 2, pp. 1185–1194.Rohling, E. J., Grant, K., Hemleben, Ch., Siddall, M., Hoogakker, B. A. A.,
1175 Bolshaw, M., Kucera, M., 2007. High rates of sea-level rise during the last interglacial period. Nature Geoscience
1176 1, 38–42

1177 Roy, P., Connell, J., 1991. Climatic-change and the future of atoll States. Journal of Coastal Research, 7, 1057–
1178 1075.

1179 Sadler, P.M., 1999. The influence of hiatuses on sedimentation accumulation rates. GeoResearch Forum 5, 15–40.

1180 Scoffin, T.P., 1993. The geological effects of hurricanes on coral reefs and the interpretation of storm deposits.
1181 Coral Reefs 10, 203–221.

1182 Seurat, L. G., 1904. Observations sur la structure, la faune et la flore de l'île de Marutea du Sud (Archipel des
1183 Tuamotu). Journal Officiel des Établissements Français d'Océanie 53, 156–161.

1184 Shope, J. B., Storlazzi, C. D., Erikson, L. H., Hegermiller, C. A., 2016. Changes to extreme wave climates of
1185 islands within the Western Tropical Pacific throughout the 21st century under RCP 4.5 and RCP 8.5, with
1186 implications for island vulnerability and sustainability. Global and Planetary Change, 141, 25–38.

1187 Shope, J. B., Storlazzi, C. D., Hoeke, R. K., 2017. Projected atoll shoreline and run-up changes in response to sea-
1188 level rise and varying large wave conditions at wake and Midway Atolls, Northwestern Hawaiian Islands.
1189 Geomorphology 295, 537–550.

1190 Shope J.B., Storlazzi, C.D., 2019. Assessing morphologic controls on atoll island alongshore sediment transport
1191 gradient due to future sea-level rise. Frontiers in Marine Science 6, 245.

1192 Sladen, A., Hebert, H., Schindele, F., Reymond, D., 2007. Evaluation off airfield tsunami hazard in French
1193 Polynesia based on historical and numerical simulations. Natural Hazards and Earth Systems Sciences 7, 195e206.

1194 Smithers, S. G., Hoeke, R. K., 2014. Geomorphological impacts of high- latitude storm waves on low-latitude reef
1195 islands – observations of the December 2008 event on Nukutoa, Takuu, Papua New Guinea. Geomorphology 222,
1196 106–121.

1197 Stephens, S.A., Ramsay, D.L., 2014. Extreme cyclone wave climate in the Southwest Pacific Ocean: influence of
1198 El Niño-Southern Oscillation and projected climate change. Global and Planetary Change 123, 13–26.

1199 Stoddart D.R., 1971. Coral reefs islands and catastrophic storms, In J.A. Steers (Ed.). Applied Coastal
1200 Geomorphology, Macmillan, London, p. 155–197.

1201 Stoddart D.R., Steers J.A., 1977. The nature and origin of coral reef islands, p. 59–105. In: O.A. Jones et R.
1202 Endean (eds.) – Biology and geology of coral reefs, Academic Press, New York, vol. 4, Geology 2.

1203 Stoddart, D.R., McLean, R.F., Hopley, D., 1978. Geomorphology of reef islands, northern Great Barrier Reef.
1204 Philosophical Transactions of the Royal Society of London B 284, 39–61.

1205 Storlazzi, C. D., Elias, E. P. L., Berkowitz, P., 2015. Many Atolls may be uninhabitable within decades due to
1206 climate change. Science Report, 5, 14546.

1207 Studholme, J., Fedorov, A.V., Gulev, S.K., Emanuel, K., Hofges, K., 2022. Poleward expansion of tropical
1208 cyclone latitudes in warming climates. Nature Geoscience 15, 14–28.

1209 Terry, J.P., Goff, J., 2014. Megaclasts: proposed revised nomenclature at the coarse end of the Udden-Wentworth
1210 grain-size scale for sedimentary particles. Journal of Sedimentary Research 84, 192–197.

1211 Terry, J.P., Etienne, S., 2011. Stones from the dangerous winds: reef platform mega-clasts in the tropical Pacific
1212 Islands. Natural Hazards 56, 567–569.

1213 Wandress, M., Aucan, J., Espejo, A., Jackson, N., De Ramon N'Yeurt, A., Damlamian, H., 2020. Distant-source
1214 swells cause coastal inundation on Fiji's coral coast. Frontiers in Marine Science 7, 546 doi:
1215 10.3389/fmars.2020.00546

1216 Webb, A. P., Kench, P. S., 2010. The dynamic response of reef islands to sea- level rise: evidence from multi-
1217 decadal analysis of island change in the Central Pacific. Global and Planetary Change 72, 234–246.

1218 Woodroffe, C.D., 2008. Reef-island topography and the vulnerability of atolls to sea-level rise. Global and
1219 Planetary Change 62, 77–96.

1220 Woodroffe, C.D., McLean, R.F., Smithers, S.G., Lawson, E.M., 1999. Atoll reef-island formation and response to
1221 sea-level change: West Island, Cocos (Keeling) Islands. Marine Geology 160, 85–104.

1222 Woodroffe, C.D., Morrison, R.J., 2001. Reef-island accretion and soil development, Makin Island, Kiribati,
1223 Central Pacific. Catena 44, 245–261.

1224 Woodroffe, C. D., Biribo, N., 2011. Atolls. In D. Hopley (Ed.), Encyclopedia of Modern Coral Reefs: Structure,
1225 Form and Process. Springer, the Netherlands, pp. 51–71.

1226 Woodruff, J.D., Irish, J.F., Camargo, S.J., 2013. Coastal flooding by tropical cyclones and sea- level rise. Nature
1227 504, 45–52.

1228 Yamano H, Kayanne H, Yamaguchi T, Kuwahara Y, Yokoki H, Shimazaki H, Chicamori M, 2007. Atoll island
1229 vulnerability to flooding and inundation revealed by historical reconstruction: Fongafale Islet, Funafuti Atoll,
1230 Tuvalu. Global and Planetary Change 57, 407–416.

1231 Yamano, H., Cabioch, G., Chevillon, C., Join, J.L., 2014. Late Holocene sea-level change and reef-island
1232 evolution in New Caledonia. Geomorphology 222, 39–45.

Yasukochi, T., Kayanne, H., Yamaguchi, T., Yamano, H., 2014. Sedimentary facies and Holocene depositional processes of Laura Island, Majuro Atoll. Geomorphology 222, 59–67.

Yates, M. L., Le Cozannet, G., Garcin, M., Salaï, E., Walker, P., 2013. Multidecadal Atoll shoreline change on Manihi and Manuae, French Polynesia. Journal of Coastal Research 289, 870–882.

Zhang, Z., Leduc, G., Sachs, J.P., 2014. El Niño evolution during Holocene revealed by a biomarker rain gauge in the Galapagos Islands. Earth Planetary Sciences Letters 40, 420–434.

Figure captions

Fig. 1. (a) Location map of South-Marutea Atoll in the Gambier Island Group, south-eastern Tuamotu Archipelago, French Polynesia, central south Pacific; (b) Google Earth map of South-Marutea Atoll showing the location of the studied site areas (boxes): Motu Aramu (see Fig. 1c), with location of excavations (star symbols); Motu Vainono (see Fig. 1d), with location of excavations (star symbols), and ocean-facing shingle-ridge profile (Fig. 4a); Motu Aranui (see Fig. 1e) with location of dated coral-clast samples (open circle symbols); Motu Oire (see Fig. 1f) with location of outer shingle-ridge profile (Fig. 4b); Motu Tekava (see Fig. 1g) with location of dated coral-clast samples (open-circle symbols).

Fig. 2. Wind rose for Mangareva site – altitude: +91 m; 23°07’48” S, 134°57’55”W –, Gambier island, south-eastern Tuamotu, showing the dominant wind directions from the north and north-east sectors. Based on records from Météo-France and reprinted with the permission of Météo-France. Data duplication and redistribution are prohibited except with the prior agreement of Météo-France.

Fig. 3. Tracks of some tropical cyclones within the south-eastern Tuamotu region since the beginning of the twentieth century. Modified from Laurent and Varney (2014).

Fig. 4. Transverse topographic profiles across outer shingle ridges of the reef- rim and islet, South-Marutea Atoll, showing the different geomorphic components. (a) south-east of Motu

Vainono – see fig. 1 d for location –; (b) west of Motu Oire – see fig. 1f for location. The location of the dated coral-clast samples is indicated. Ages are given in years before present (before 2022). See Table 1 for dating parameters.

Fig. 5. Conglomerate platforms from the reef rim, South-Marutea Atoll; (a) overview of the two-layer, 1.10 m thick conglomerate pavement, hoa side, south of Motu Oire; (b) close-up picture of the 1.20 m thick conglomerate bed, reef-flat side, west of Motu Oire – see fig. 1f for location –; (c) close-up picture of the two-layer, 1.20 m thick conglomerate pavement, west of Motu Aranui – see fig. 1b and 1e for location. The location of the dated coral-clast samples is indicated. Ages are given in years before 2022. See Table 1 for details on dating parameters.

Fig. 6. Aerial view of the south-south-east side of Motu Vainono, southern reef-rim area of South-Marutea Atoll, showing, from the ocean landwards, the reef-flat zone, about 200 m wide, the conglomerate-platform front line (brown colour), the outer beach (white colour), the successive shingle ridges (grey colour) and the vegetation-covered islet bench. See fig. 1d for location and fig. 4a for geomorphic profile.

Fig. 7. Close-up picture of the upper part of the ocean-facing shingle ridge, composed of blocky, pocilloporid and acroporid coral clasts, south-east of Motu Vainono, southern reef-rim area, South-Marutea Atoll.

Fig. 8. Transverse topographic profile across Motu Aramu, north-north-eastern reef-rim area, South-Marutea Atoll, showing the location and lithostratigraphy of excavations A, B and C, with location and radiometric ages of the dated coral-clast samples. See figure 1b, c for location of excavations and Table 1 for dating parameters. Ages are given in calendar years

– relative to 2022, the year of analysis. See Table 1 (Supplementary material) for details on dating parameters. WL: water-table level.

Fig. 9. Transverse topographic profile across Motu Vainono, south-south-western rim area, South-Marutea Atoll, showing the location and lithostratigraphy of excavations D, E and F, with location and radiometric ages of the dated coral-clast samples. See fig. 1b, d for location of excavations and Table 1 for dating parameters. Ages are given in calendar years (relative to 2022. the year of analysis). See Table 1 (Supplementary material) for details on dating parameters. WL: water-table level.

Fig. 10. Plot of the U/Th dated coral-clast samples *versus* their respective topographic or stratigraphic location across or within the studied motu sites – see figs. 1b to 1g, 4a, 4b, 8 and 9 for location. Ages are given in calendar years (relative to 2022, the year of analysis). Vainono excavations: note the decreasing age trend from the ocean-facing islet side lagoonwards. Aramu excavations: note a similar, but less continuous age decreasing trend, due to both younger clast deposits at the ocean-facing islet site and hiatus in clast supply between 4,000 and 2,000 calendar yr.

Fig. 11. Views of the internal structure and lithostratigraphy of the sedimentary piles, from excavations through Motu Aramu and Motu Vainono, respectively; (a) Excavation A, ocean-facing islet margin, showing the upper 1 m section, composed of pebble-dominated, sand supported material; (b) Excavation C, lagoon-facing islet margin, showing the whole section, composed of sand-dominated, pebble-rich sediments, overtopped by a dark, organic bed. The level of the water table is about 0.20 m above the excavation bottom; (c) excavation D, ocean-facing islet margin, showing the lower section composed of cobble-to pebble-dominated, sand to pebble-supported detritus. The level of the water table is about 0.10 m above the

excavation bottom; (d) excavation F, lagoon-facing margin, showing the whole section, composed of sand-dominated, pebble-rich material. The top section exhibits an about 0.50 m thick organic deposit. The level of the water table is about 0.25 m above the excavation bottom.

Fig. 12. Relationships between the main islet accretional phases on South-Marutea Atoll, regional changes in sea level and in ENSO-controlled cyclogenesis over the past 5,000 years; (a) accretional phases at Aramu and Vainono sites, based on the number of dated coral-clast samples; (b) regional sea level curve, modified from Pirazzoli and Montaggioni (1987), and Hallmann et al. (2020); (c) record of ENSO activity based on measurement of sand percentage in Juna Crater Lake, Galapagos, modified from Conroy et al., 2008; (d) record of ENSO activity based on sediment laminae light-intensity from a core extracted from Laguna Pallcacocha, Ecuador, modified from Moy et al., 2002.

Fig. 13. Cross-section through Motu Aramu, north-eastern rim area, South-Marutea Atoll, showing the successive phases of islet accretion. The dashed lines refer to accretion isochrons, given in years before present and are defined from time intervals between the dated coral-clast samples. Are indicated the location of the excavation and of the dated coral samples extracted from conglomerates.

Fig. 14. Cross-section through Motu Vainono, southern rim area, South-Marutea Atoll, showing the successive phases of islet accretion. The dashed lines refer to accretion isochrons, given in years before present and are defined from time intervals between the dated coral-clast samples. The location of the excavation and of the dated coral samples extracted from conglomerates are indicated.

Fig. 15. View of the south-east-facing, outer shingle ridge, Motu Tekava, east-south-eastern rim area, South-Marutea Atoll, clearly showing that coral-clast deposits are in process of rapid cementation, probably under the control of percolating vadose fresh waters.

Fig. 16. Planimetric reconstruction of Motu Aramu (north-eastern rim area) and Motu Vainono (southern rim area), South-Marutea Atoll, showing the expected successive phases of islet accretion over the last 5,000 years. Isochrons delineate the expected surface areas of initial depocentres and incipient islets through time. Interrogation points relate to the younger accretional sections from which there are insufficient age records. From 5,000 to about 3,000 calendar yr at Aramu and from 5,000 to about 1,500 calendar yr at Vainono, spaces between adjacent depocentres and incipient islets are interpreted to have acted as hoa prior to have been sealed.

Fig. 17. Age distribution of identified wave-surge events over the last 5,000 years, based on U/Th dating of coral-clast samples extracted from conglomerate platforms, islet excavations and surficial deposits. The last 2,000 years, i.e. the Common Era, is also expressed in a centurial scale to facilitate comparison between the historical record of marine hazard events and the wave-surge events recorded in the present study.

Table 1 (Supplementary material)

Uranium–Thorium data of coral samples from South-Marutea Atoll. Are given successively laboratory sample codes, field sample (SAT) numbers, uranium and thorium contents, isotopic composition with statistical errors – two standard deviations of the mean – and ages. Uranium and thorium contents and isotopic ratios. $\delta^{234}U_M = \{[(^{234}U/^{238}U)_{sample}/(^{234}U/^{238}U)_{eq}]-1\} \times 1000$, where $(^{234}U/^{238}U)_{sample}$ is the measured atomic ratio and $(^{234}U/^{238}U)_{eq}$ is the atomic ratio at secular equilibrium. $\delta^{234}U_{(T)}$ is the initial value and is calculated by the equation:

1347 $\delta^{234}U_{(0)} = \delta^{234}U_{meas} \exp^{(\lambda 234t)}$, where t is the age in years and λ_{234} is the decay constant for
1348 ^{234}U. Ages were corrected for authigenic ^{230}Th using $^{230}Th/^{232}Th$) of the detrital fraction = 10
1349 ± 5. Note that, for Samples M103, M123 and M129, uranium content is significantly lower
1350 than classical values for uranium content within aragonitic corals. M103 is a conglomerate
1351 and not massive coral. Calcite primary deposition could explain the low U content value for
1352 this sample. For Samples M123 and M129, the very low U content could be a clue of
1353 diagenetic alteration (with U loss during the well-known aragonite to calcite transformation).
1354 These two ages could be considered with caution, because a hypothetical U loss could have
1355 biased the relevant age (with an apparent age being too old). Ages are expressed in both
1356 calendar years, relative to the year of sample analysis (2022) corrected for detrital content
1357 using a $^{230}Th/^{232}Th$ isotopic ratio = 7 ± 50 % and conventional ages BP (Before Present,
1358 relative to 1950).

1359


(a)
South Pacific Ocean
MARQUESAS ISLANDS
TUAMOTU ISLANDS
SOCIETY ISLANDS
AUSTRAL ISLANDS
GAMBIER ISLANDS
FRENCH POLYNESIA
Takapoto
Manihi
Taha'a
Rangiroa
Makemo
Moorea
Tahiti
Anaa
Hao
Marutea Sud
Tureia
Mororoa
Mangareva
10°S
20°S
200 km
150°W
140°W
(b)
135°37'W
135°29'W
N
OIRE
Fig.1F
ARAMU
Fig.1C
21°30'S
MARUTEA SUD
ARANUI
Fig.1E
Fig.1G
TEKAVA
21°33'S
Fig.1D
VAINONO
2 km
(c)
Fore-reef zone
Conglomerate platform
Reef flat zone
MOTU ARAMU
Hoa
Lagoon
100 m
(d)
Lagoon
Hoa
MOTU VAINONO
Fig. 4a
Reef flat zone
Shingle ridge
200 m
(e)
MOTU ARANUI
Lagoon
M135
M137
M140
M138
Conglomerate platform
Reef flat zone
Hoa
80 m
(f)
Conglomerate Platform
MOTU OIRE
Reef flat zone
Fig. 4b
Shingle ridge
40 m
(g)
MOTU TEKAVA
M109
Hoa
M100
M103
M104
M107
M101
M102
Conglomerate platform
Reef flat zone
200 m

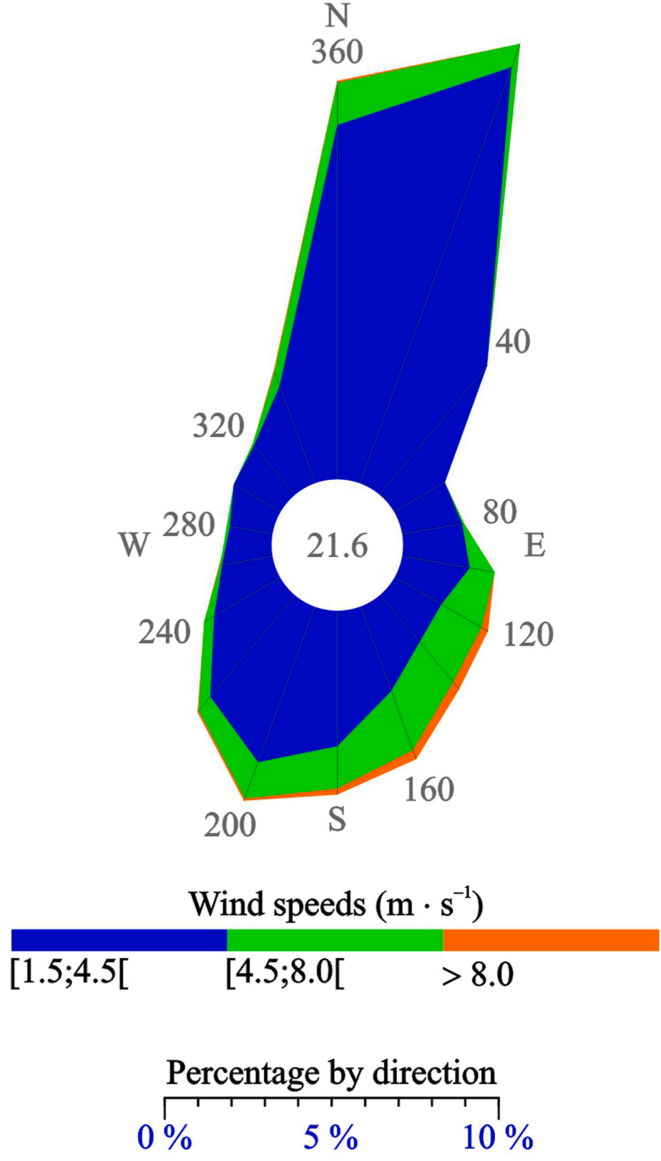
N
360
40
80
E
120
160
S
200
240
W
280
320
21.6
Wind speeds (m · s⁻¹)
[1.5;4.5[
[4.5;8.0[
> 8.0
Percentage by direction
0 %
5 %
10 %

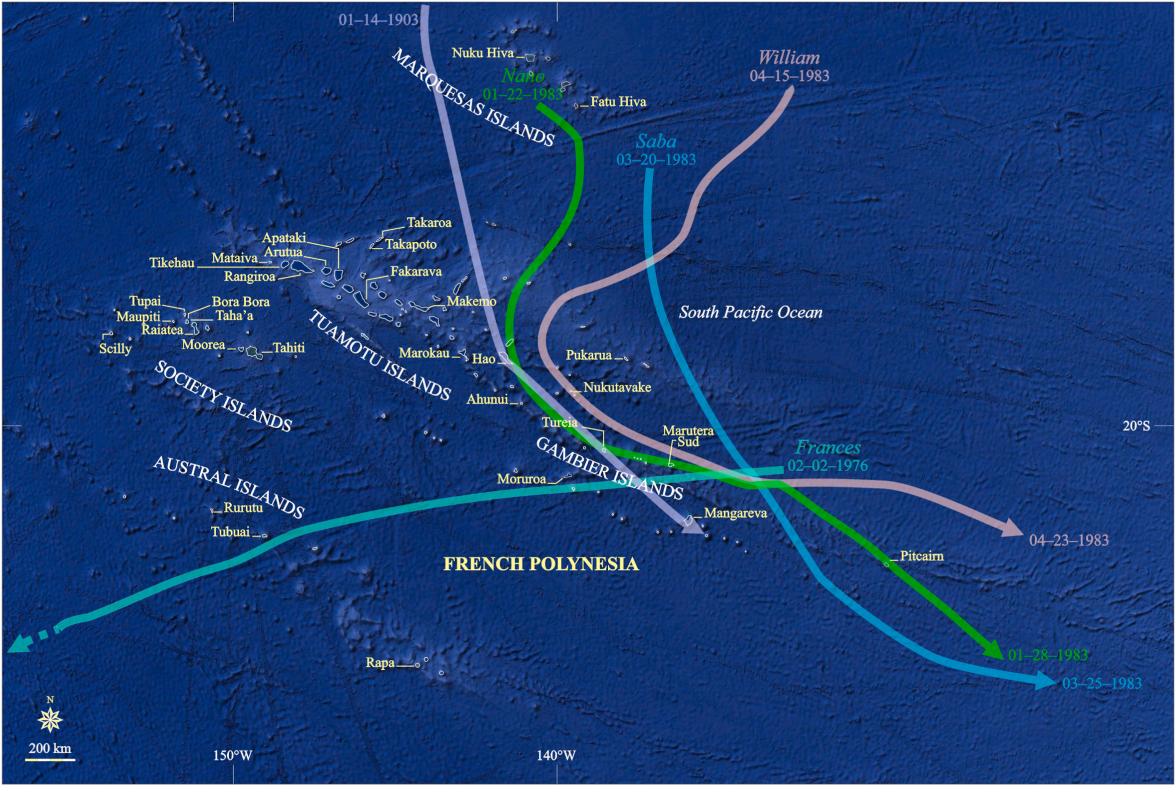
01–14–1903
Nuku Hiva
MARQUESAS ISLANDS
Nora
01–22–1983
Fatu Hiva
William
04–15–1983
Saba
03–20–1983
Takaroa
Apataki
Takapoto
Tikehau
Mataiva
Arutua
Rangiroa
Fakarava
Tupai
Bora Bora
Maupiti
Taha'a
Raiatea
Makemo
South Pacific Ocean
Scilly
Moorea
Tahiti
TUAMOTU ISLANDS
Marokau
Hao
Pukarua
Nukutavake
SOCIETY ISLANDS
Ahunui
Tureia
Marutera Sud
20°S
Frances
02–02–1976
GAMBIER ISLANDS
AUSTRAL ISLANDS
Moruroa
Rurutu
Tubuai
Mangareva
04–23–1983
Pitcairn
FRENCH POLYNESIA
01–28–1983
03–25–1983
Rapa
N
200 km
150°W
140°W

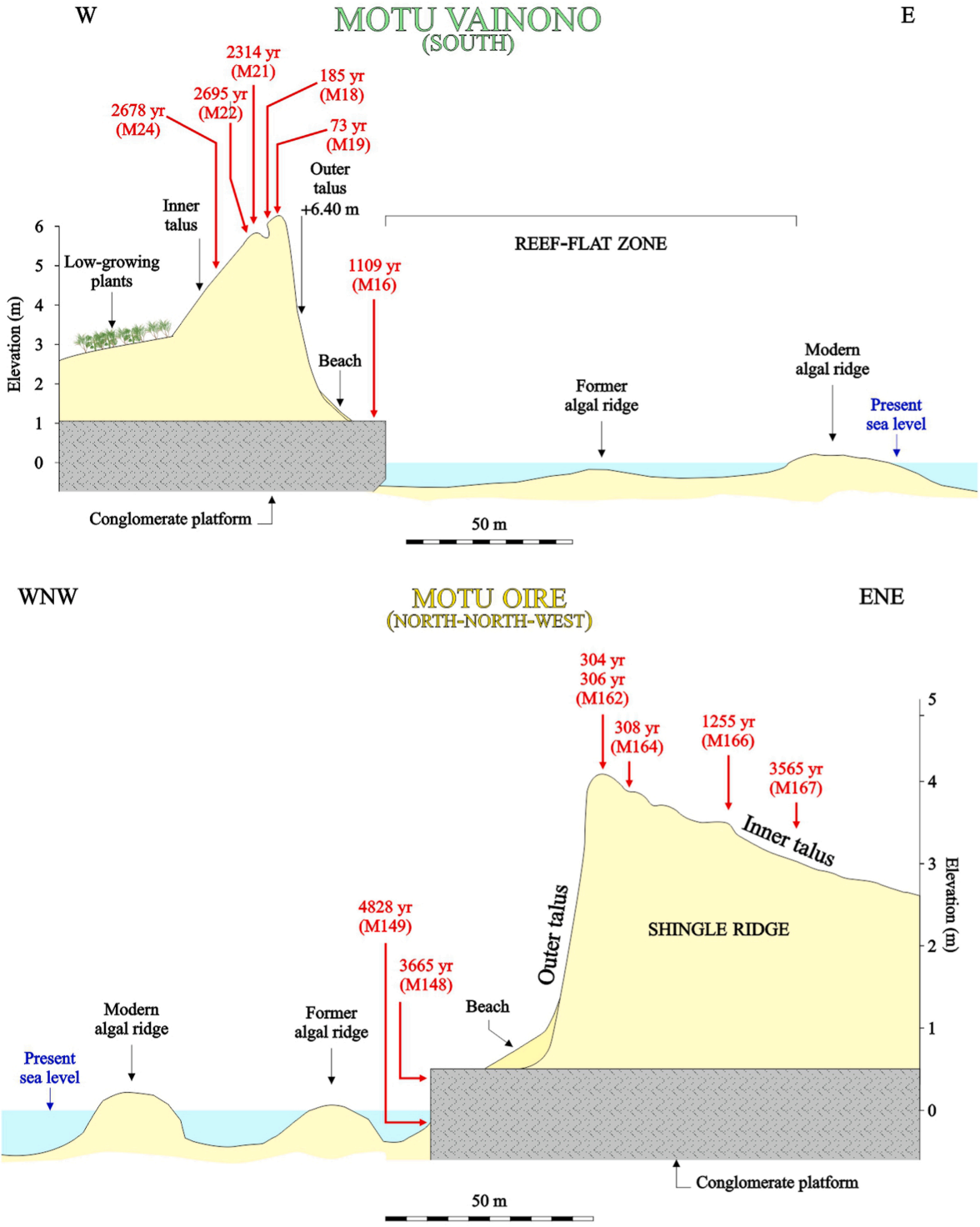
W
MOTU VAINONO
(SOUTH)
E
2314 yr
(M21)
2695 yr
(M22)
2678 yr
(M24)
185 yr
(M18)
73 yr
(M19)
Outer
talus
+6.40 m
Inner
talus
REEF-FLAT ZONE
Low-growing
plants
1109 yr
(M16)
Elevation (m)
6
5
4
3
2
1
0
Beach
Modern
algal ridge
Former
algal ridge
Present
sea level
Conglomerate platform
50 m
WNW
MOTU OIRE
(NORTH-NORTH-WEST)
ENE
304 yr
306 yr
(M162)
308 yr
(M164)
1255 yr
(M166)
3565 yr
(M167)
Inner talus
Outer talus
SHINGLE RIDGE
4828 yr
(M149)
3665 yr
(M148)
Beach
Modern
algal ridge
Former
algal ridge
Present
sea level
Elevation (m)
5
4
3
2
1
0
Conglomerate platform
50 m

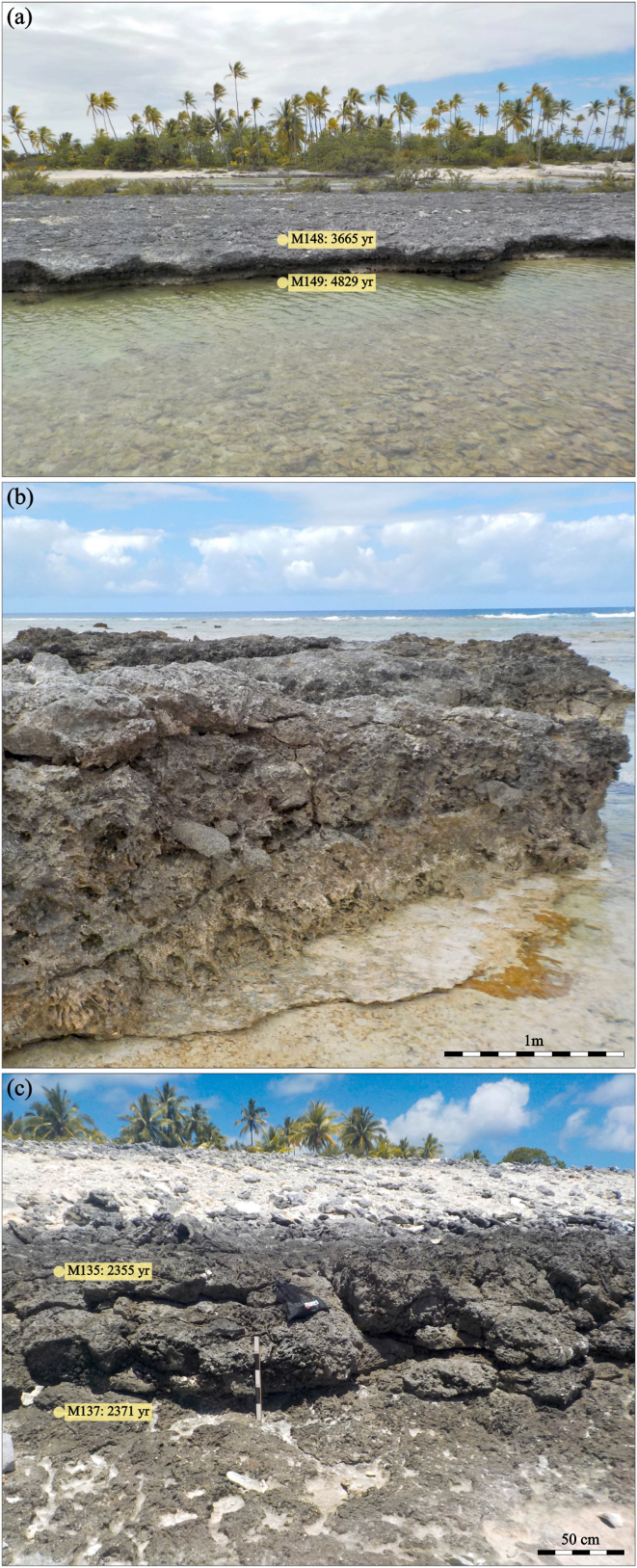
(a)
M148: 3665 yr
M149: 4829 yr
(b)
1m
(c)
M135: 2355 yr
M137: 2371 yr
50 cm

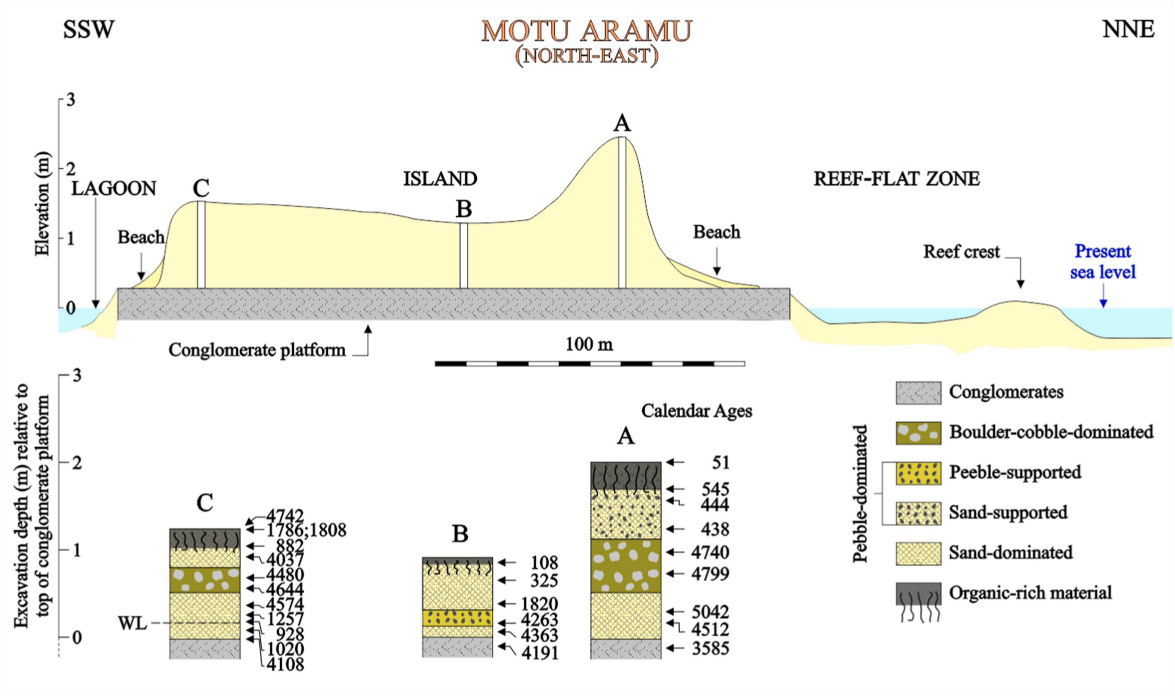
SSW
MOTU ARAMU
(NORTH-EAST)
NNE
Elevation (m)
3
2
1
0
LAGOON
C
ISLAND
A
B
REEF-FLAT ZONE
Beach
Beach
Reef crest
Present sea level
Conglomerate platform
100 m
Excavation depth (m) relative to top of conglomerate platform
Calendar Ages
C
4742
1786;1808
882
4037
4480
4644
4574
1257
928
1020
4108
WL
B
108
325
1820
4263
4363
4191
A
51
545
444
438
4740
4799
5042
4512
3585
Conglomerates
Boulder-cobble-dominated
Peeble-supported
Sand-supported
Pebble-dominated
Sand-dominated
Organic-rich material

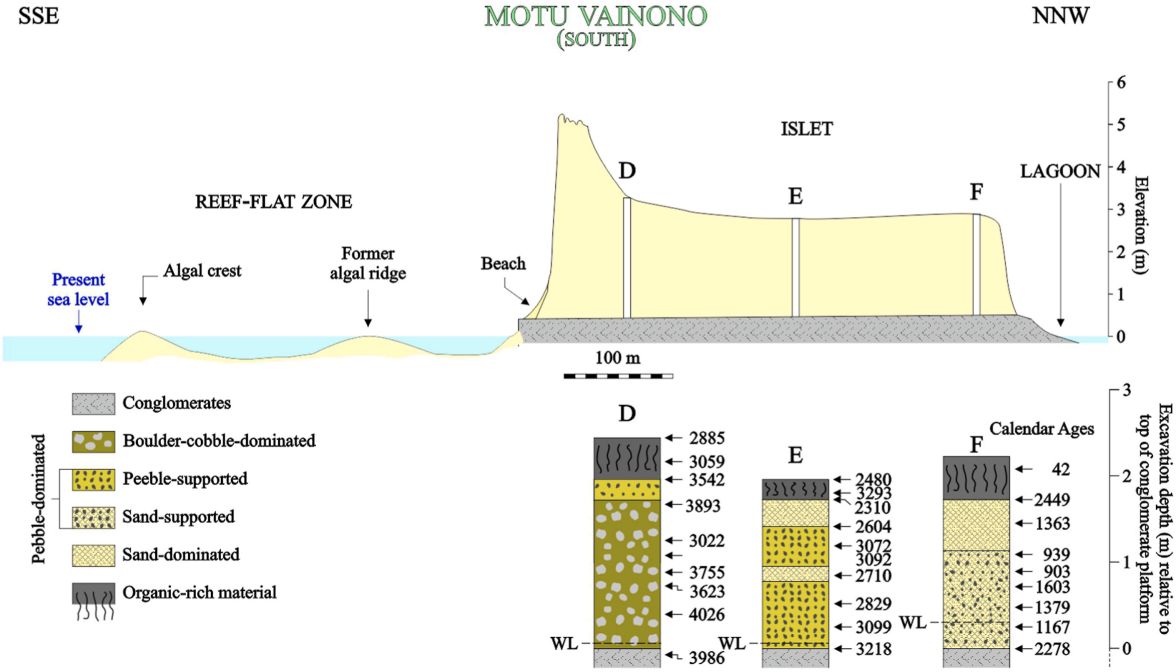
SSE
MOTU VAINONO
(SOUTH)
NNW
ISLET
D
E
F
LAGOON
REEF-FLAT ZONE
Present sea level
Algal crest
Former algal ridge
Beach
Elevation (m)
100 m
Conglomerates
Boulder-cobble-dominated
Peeble-supported
Sand-supported
Sand-dominated
Organic-rich material
Pebble-dominated
Calendar Ages
2885
3059
3542
3893
3022
3755
3623
4026
WL
3986
2480
3293
2310
2604
3072
3092
2710
2829
3099
3218
42
2449
1363
939
903
1603
1379
1167
2278
Excavation depth (m) relative to top of conglomerate platform

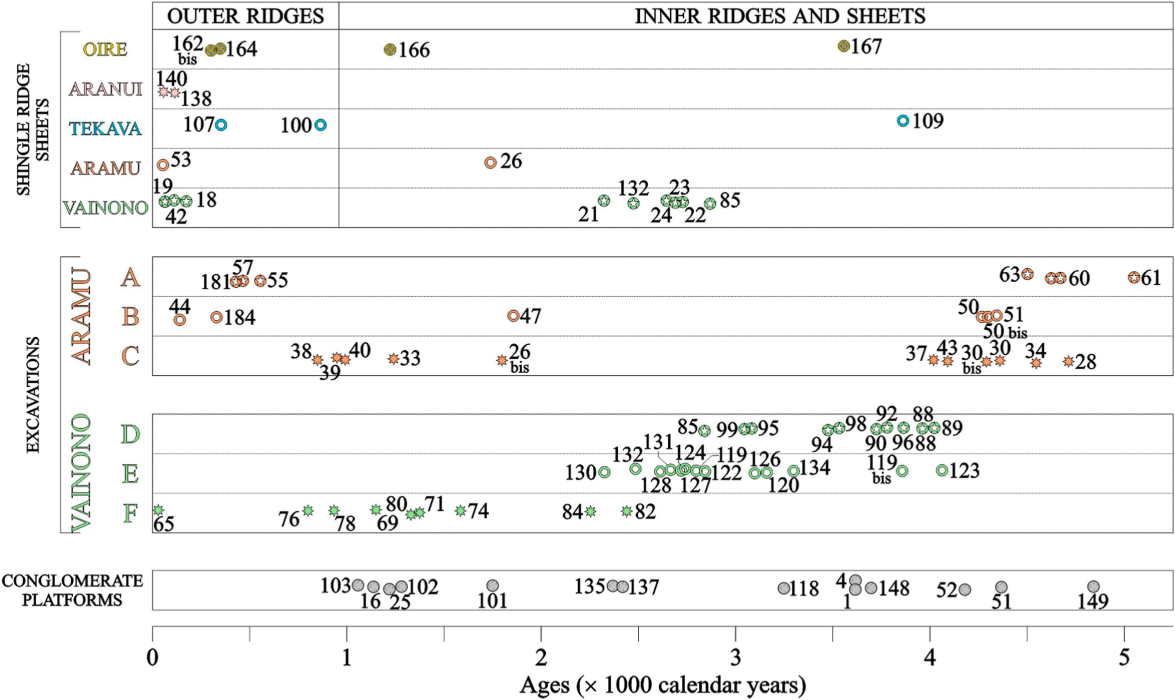
OUTER RIDGES
INNER RIDGES AND SHEETS
SHINGLE RIDGE SHEETS
OIRE
ARANUI
TEKAVA
ARAMU
VAINONO
162 bis
164
166
167
140
138
107
100
109
53
26
19
18
42
132
23
21
24
22
85
EXCAVATIONS
ARAMU
A
B
C
57
181
55
63
60
61
44
184
47
50
51
50 bis
38
40
39
33
26 bis
37
43
30 bis
30
34
28
VAINONO
D
E
F
85
99
95
98
92
88
89
94
90
96
88
132
131
124
119
126
130
122
134
119 bis
123
128
127
120
65
76
78
69
80
71
74
84
82
CONGLOMERATE PLATFORMS
103
16
25
102
101
135
137
118
4
1
148
52
51
149
0
1
2
3
4
5
Ages (× 1000 calendar years)

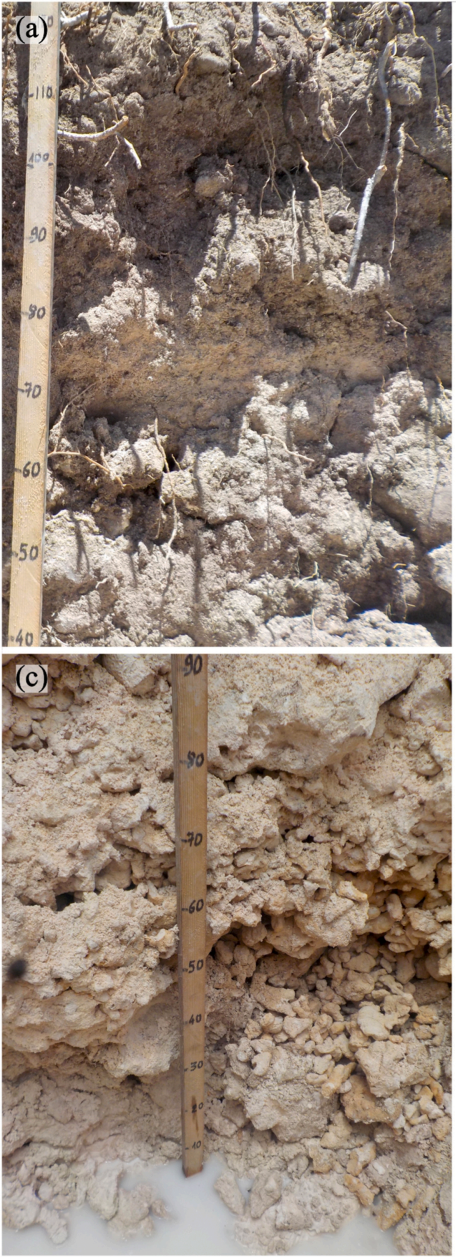
(a)
(b)
(c)
(d)

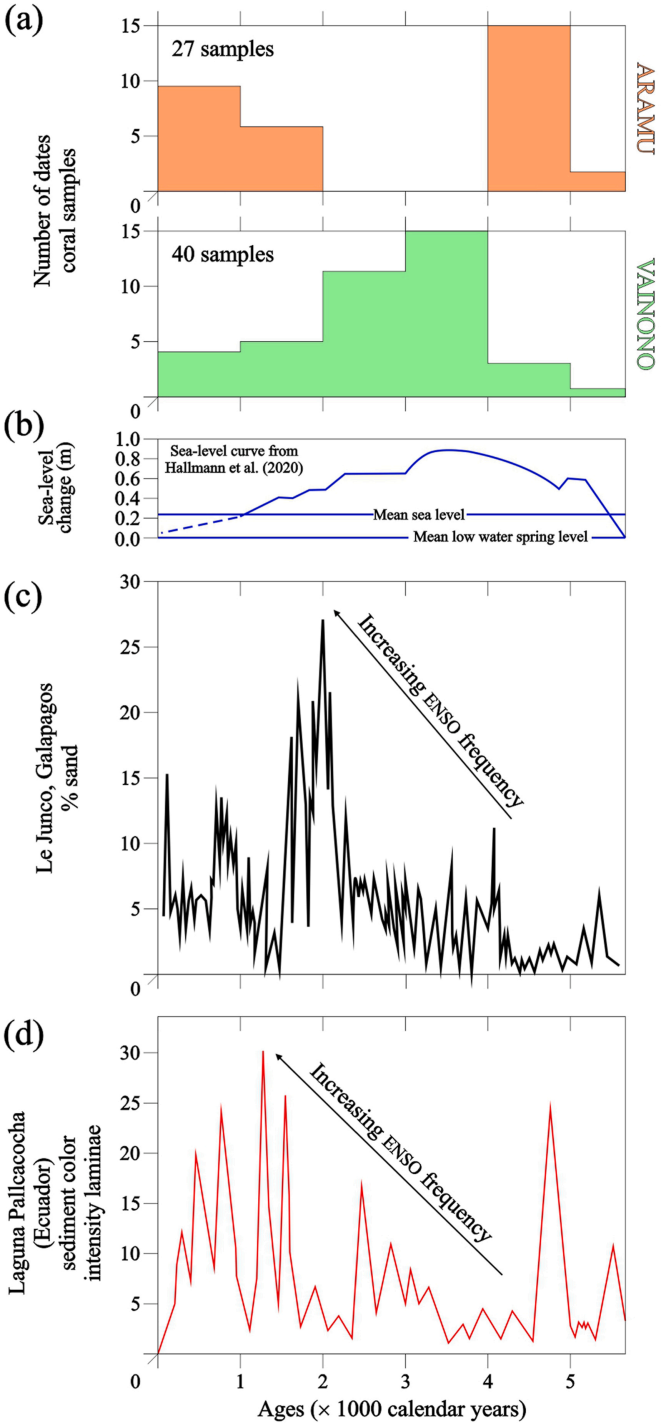
(a)
27 samples
ARAMU
40 samples
VAINONO
Number of dates coral samples
(b)
Sea-level change (m)
Sea-level curve from Hallmann et al. (2020)
Mean sea level
Mean low water spring level
(c)
Le Junco, Galapagos % sand
Increasing ENSO frequency
(d)
Laguna Pallcacocha (Ecuador) sediment color intensity laminae
Increasing ENSO frequency
Ages (× 1000 calendar years)

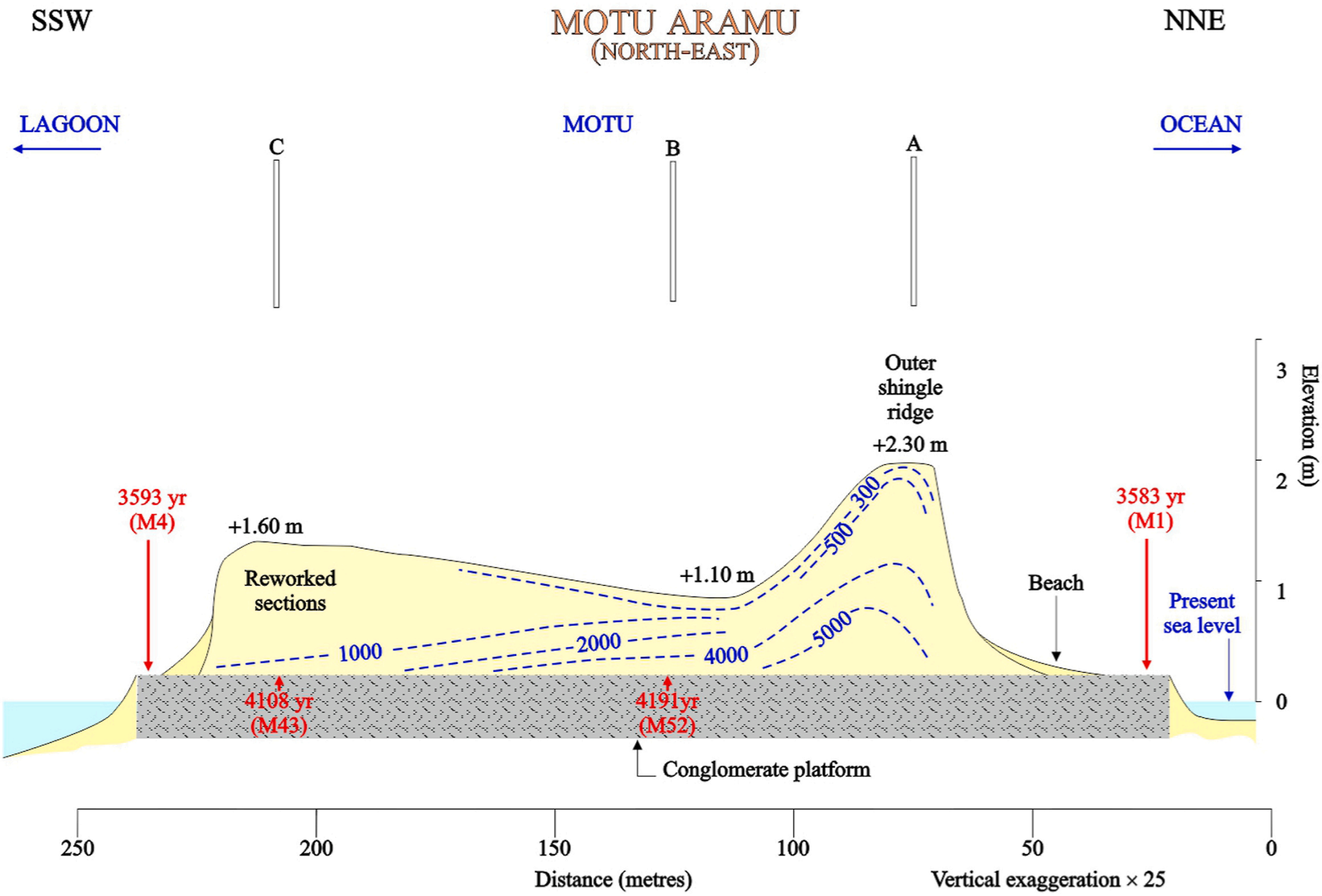
SSW
MOTU ARAMU
(NORTH-EAST)
NNE
LAGOON
MOTU
OCEAN
C
B
A
Outer
shingle
ridge
+2.30 m
3593 yr
(M4)
+1.60 m
Reworked
sections
+1.10 m
3583 yr
(M1)
Beach
Present
sea level
1000
2000
4000
300
500
5000
4108 yr
(M43)
4191yr
(M52)
Conglomerate platform
Elevation (m)
3
2
1
0
250
200
150
100
50
0
Distance (metres)
Vertical exaggeration × 25

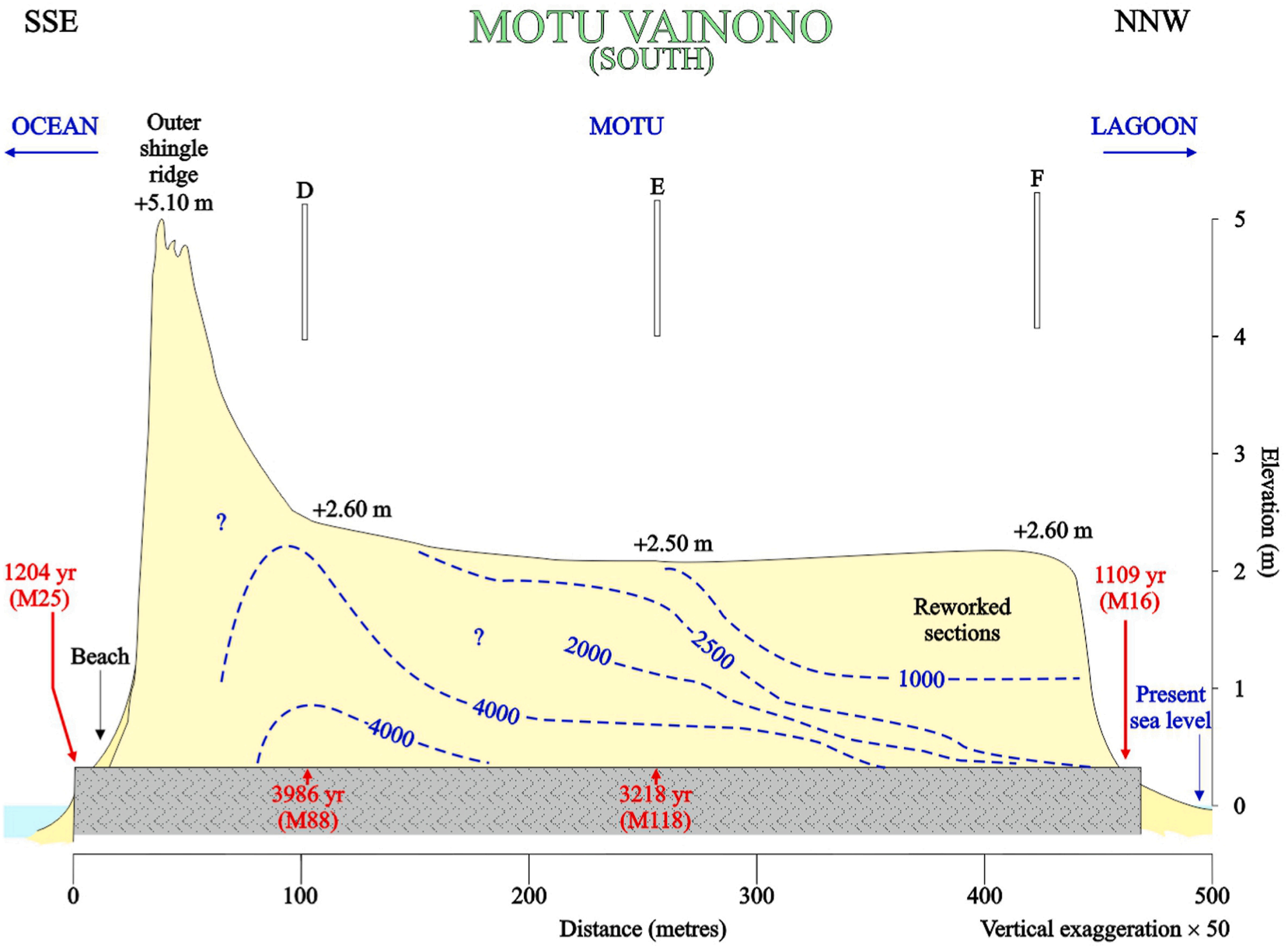
SSE
MOTU VAINONO
(SOUTH)
NNW
OCEAN
Outer
shingle
ridge
+5.10 m
MOTU
LAGOON
D
E
F
+2.60 m
+2.50 m
+2.60 m
?
?
1204 yr
(M25)
Beach
1109 yr
(M16)
Reworked
sections
2000
2500
1000
4000
4000
Present
sea level
3986 yr
(M88)
3218 yr
(M118)
Elevation (m)
5
4
3
2
1
0
0
100
200
300
400
500
Distance (metres)
Vertical exaggeration × 50


M102: 1339 yr
M101: 1743 yr

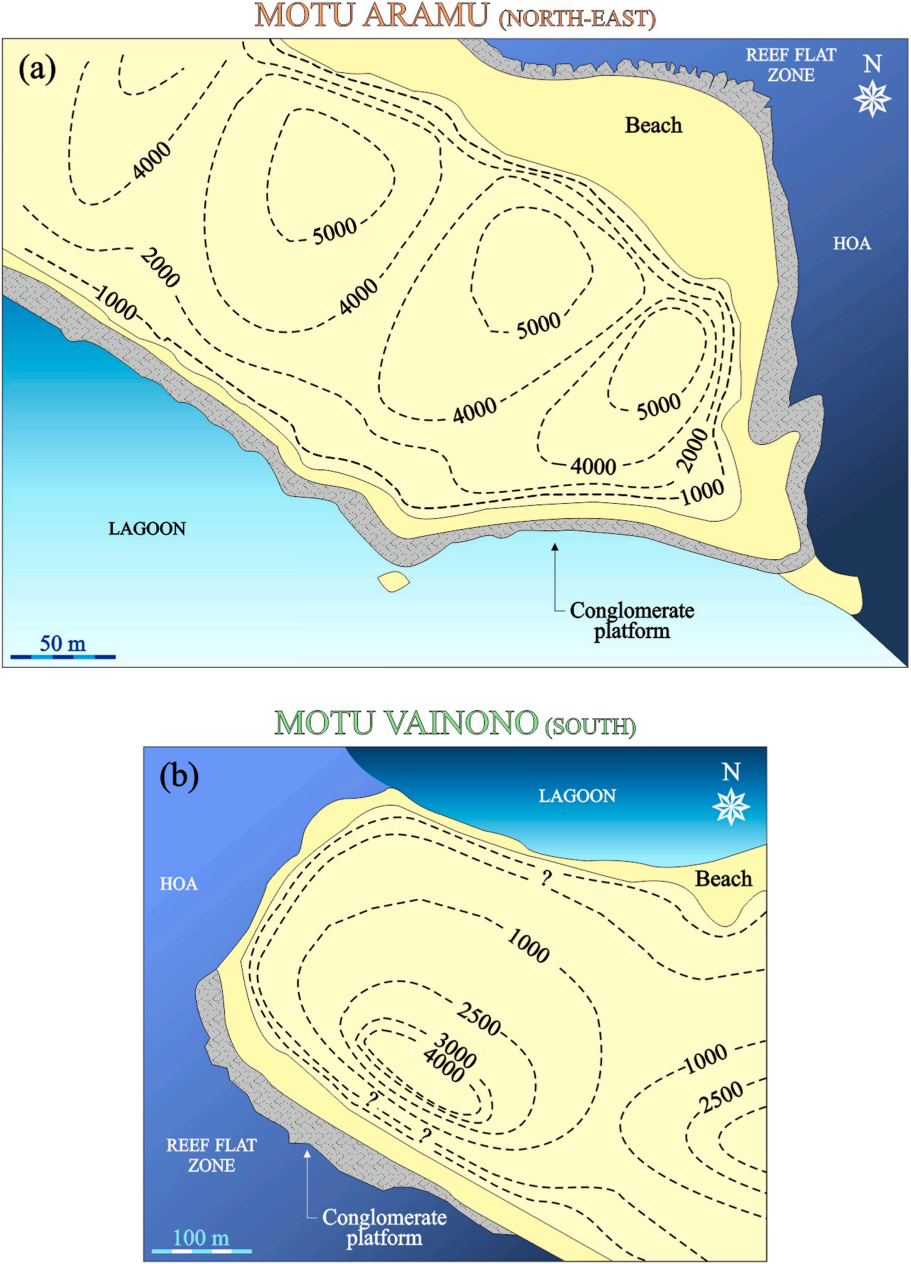
MOTU ARAMU (NORTH-EAST)
(a)
REEF FLAT ZONE
N
Beach
HOA
4000
5000
2000
1000
4000
5000
4000
5000
4000
2000
1000
LAGOON
Conglomerate platform
50 m
MOTU VAINONO (SOUTH)
(b)
LAGOON
N
HOA
Beach
?
1000
2500
3000
4000
?
?
1000
2500
REEF FLAT ZONE
Conglomerate platform
100 m

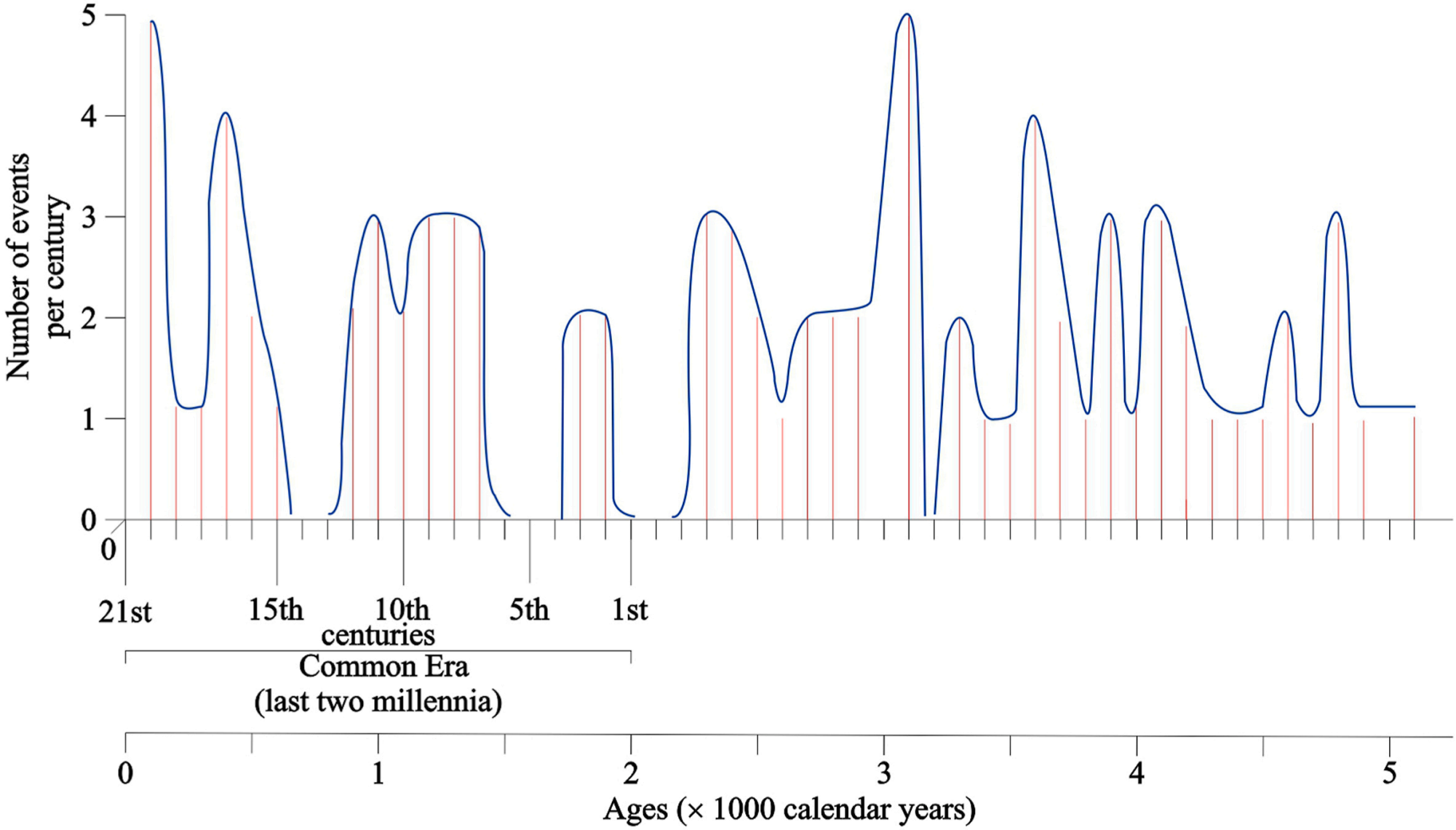
Number of events per century
5
4
3
2
1
0
0
21st
15th
10th
5th
1st
centuries
Common Era
(last two millennia)
0
1
2
3
4
5
Ages (× 1000 calendar years)

HIGHLIGHTS

- North of Rangiroa Atoll, due to a former uplift, the top of the Miocene carbonate basement peaks at depths of less than 10 m beneath the modern reef-rim surface.
- Unusual, extreme marine hazard events were essential drivers of early atoll rim-island accretion.
- Island accretion started by about 6,000 calendar years, 3,500 years before it did in nearby subsiding atolls.